REPUBLIC OF TÜRKIYE

ALTINBAŞ UNIVERSITY

Institute of Graduate Studies

Electrical and Computer Engineering Department

USE OF ARTIFICIAL INTELLIGENCE TECHNIQUES TO IMPROVE THE PERFORMANCE OF MASSIVE MIMO AND BEAM FORMING ACCORDING TO CHANNEL ESTIMATION

Hayder SAEMARI

Master's thesis

Supervisor

Prof. Dr. Hasan Hüseyin BALIK

Istanbul, 2022

USE OF ARTİFİCİAL INTELLİGENCE TECHNİQUES TO IMPROVE THE PERFORMANCE OF MASSİVE MIMO AND BEAM FORMİNG ACCORDİNG TO CHANNEL ESTİMATİON

Hayder SAEMARI

Electrical and Computer Engineering Department

Master's thesis

ALTINBAŞ UNIVERSITY

2022

The thesis titled USE OF ARTIFICIAL INTELLIGENCE TECHNIQUES TO IMPROVE THE PERFORMANCE OF MASSIVE MIMO AND BEAM FORMING ACCORDING TO CHANNEL ESTIMATION prepared by HAYDER ABDULRIDHA JASIM SAEMARI and submitted on 12 / 2022 16 / has been **accepted unanimously** for the degree of Master of Science in Electrical and Computer Engineering .

_____

Prof. Dr. Hasan Hüseyin BALIK

the Supervisor

Thesis Défense Committee Members:

Prof Dr. Hasan Hüseyin BALIK Department of Computer Engineering

Yildiz Technique University

_____

Dr. Ögr. Üyesi Oguz ATA Department of Software Engineering

Altinbas University _____

Dr. Ögr. Üyesi Aytug BOYACI Department of Computer Engineering

National Defense University _____

I hereby declare that this thesis/dissertation meets all format and submission requirements of a Master's thesis.

Submission date of the thesis to Institute of Graduate Studies: ___/___/__

I hereby declare that all information/data presented in this graduation project has been obtained in full accordance with academic rules and ethical conduct. I also declare all unoriginal materials and conclusions have been cited in the text and all references mentioned in the Reference List have been cited in the text, and vice versa as required by the abovementioned rules and conduct.

Hayder Abdulridha Jasim SAEMARI

Signature

ACKNOWLEDGMENTS

I would like to thank my supervisor professor Dr. Hasan Hüseyin BALIK for all support during my study. It’s great pleasure to express my deepest gratitude to my friends who have shared with me best moments during my study for the master’s degree. Encouraging me during this study

ABSTRACT

USE OF ARTİFİCİAL INTELLİGENCE TECHNİQUES TO IMPROVE THE PERFORMANCE OF MASSİVE MIMO AND BEAM FORMİNG ACCORDİNG TO CHANNEL ESTİMATİON

Saemari, Hayder

M.Sc., Electrical and Computer Engineering, Altınbaş University

Supervisor: Prof. Dr. Hasan Hüseyin BALIK

Date: 12/2022

Pages: 83

Many problems that traditional algorithms cannot address have been solved by artificial intelligence, and while some benefits have been achieved by learning certain elements of the receiver, the optimal strategy is joint learning of the entire receiver, which has also been effectively used in radio communications. In order to do this, we propose a completely deep convolutional neural network that implements the receiver pipeline from the frequency domain signal stream to the encoded bits in a 5G compatible manner. By generating the inputs of the convolutional neural network in a highly accurate manner using both experimental data and code, we enable channel estimates. In addition, the soft bits produced by the deep convolutional neural network are compatible with the channel coding used in 5G systems. We show that the performance of Rx-NN is better than traditional techniques using 3GPP specific channel models. We further show that the improved performance is probably due to the ability of Rx-NN to learn to exploit known constellation locations to obtain obscure data symbols along with local symbol distribution to enhance detection accuracy, and by investigating end-to-end learning gains using a frequency and time-selective fading channel using OFDM, this is through modulation improvements that appear on AWGN channels when there is an incomplete channel in the receiver. We believe that the learned transceiver is effective because it can eliminate the need for pilots signal and remove the burden associated with demodulation signals.

Keywords: Massive MIMO, 5G, Artificial Inelegance, Neural Receiver, Channel Estimation, End-to-End system.

TABLE OF CONTENTS

Pages

LIST OF TABLES

Pages

LIST OF FIGURES

Pages

ABBREVIATIONS

AI	:	Artificial Intelligence
ML	:	Machine Learning 1G First Generation
DL	:	Deep Leaning
LSTM	:	Long-term memory networks
RNN	:	Recurrent Neural Networks
DNN	:	Deep Neural Networks
GRU	:	Gated Recurrent Unit
ITU	:	International Telecommunication Union
3GPP	:	3rd Generation Partnership Project
4G	:	Fourth Generation
5G	:	Fifth Generation
CSI	:	Channel state information
CDL	:	Cluster Delay Line
TDL	:	Tapped Delay Line
QAM	:	Quadrated amplitude modulation
FFT	:	Fast Fourier Transform
IFFT	:	Inverse Fast Fourier Transform

BS	:	Base Station
AoA	:	Angle-of-Arrival
DoA	:	Direction-of-Arrival
DoD	:	Direction-of-Departure
LDAMP	:	Learned De-Noising-Based Approximate Message Passing
MS	:	Mobile Station
DL	:	Downlink
URLLC	:	Ultra-Reliable Low-Latency Communication
SDN	:	Software-Defined Network
NVF	:	Virtual Network Functions
RAN	:	Radio Access Network
SON	:	Self-Organization Network
eMBB	:	Enhanced Mobile Broadband
FDD	:	Frequency Division Duplex
TDD	:	Time Division Duplex
ISI	:	Inter Symbol Interference
ZF	:	Zero Forcing
gNB	:	Fifth Generation Node Base station
IoT	:	Internet of Things

LOS	:	Line Of Sight
LTE	:	Long Term Evolution
LTE-A	:	Long Term Evolution - Advanced
MIMO	:	Multiple Input Multiple Output
BF	:	Beam-Forming
Mmtc	:	Massive Machine-Type Communications
MmWave	:	Millimeter Wave
NLOS	:	Non-Line of Sight
NR	:	New Radio
OFDM	:	Orthogonal Frequency Division Multiplexing
CP	:	Cyclic prefix
NOMA	:	NON-orthogonal multiplexing
AWGN	:	Additive White Gaussian Noise
PBCH	:	Physical Broadcast Channel
MMSE	:	Minimum Mean Square Error
LLRs	:	Log-Likelihood Ratios
LS	:	Liner Square
TTI	:	Transmission Time Interval
SVM	:	Support Vector Machines

LDPC	:	Low Density Parity Chick
FEC	:	Forward Correction Codes
VNDs	:	Variable Node Decoders
CND	:	Check Node Decoder
PMD	:	Probability of Misdetection
RF	:	Radio Frequency
Rx	:	Receive
Tx	:	Transmit
SCS	:	Sub Carrier Spacing
SNR	:	Signal to Noise Ratio
BER	:	Bit Error Rate
UE	:	User Equipment

1. INTRODUCTION

Wireless communications appeared commercially in the late 1977 when the first types of devices were produced, which were of the analog type and were working with AMPS technology in North America and Europe. For wireless communications (voice only) and it had little coverage and low reliability, after that the second generation of communications appeared, in which digital signals were used, through which the sound quality was improved and the coverage of larger areas and high security and the use of SMS service. Examples This generation in Europe is GSM and in North America CDMA and in the third generation and with the emergence of data traffic and the rate of transmit and receiving data more and the production of smart devices, examples of this generation are HSPA and HSPA + (mobile data), in the 4G of communications and with the emergence of LTE and LTE ADVANCED (broad band) systems [1]. which were characterized by a higher data transfer rate and in the (5G), As shown in the (Figure 1.1), which came due to the rise in the number of gadgets a services provided and the quality of communications that you need Data sent per second (from 0 to 10 Gbps) and Massive Machine-Type Communications (MMTS) is the use of a large number of connected devices and Ultra-Reliable Low-Latency Communication (URLLC) is the low latency of the connection. When we talk about the generations of wireless communications, we must refer to the international organizations and institutions that are based on issuing standards, which are a set of instructions that all companies must follow when they manufacture new technologies and the goal is to make devices from different companies deal with each other and in communications Wireless The so-called International Telecommunication Union (ITU), a body connected to the United Nations, is in charge of establishing the rules that businesses must follow.

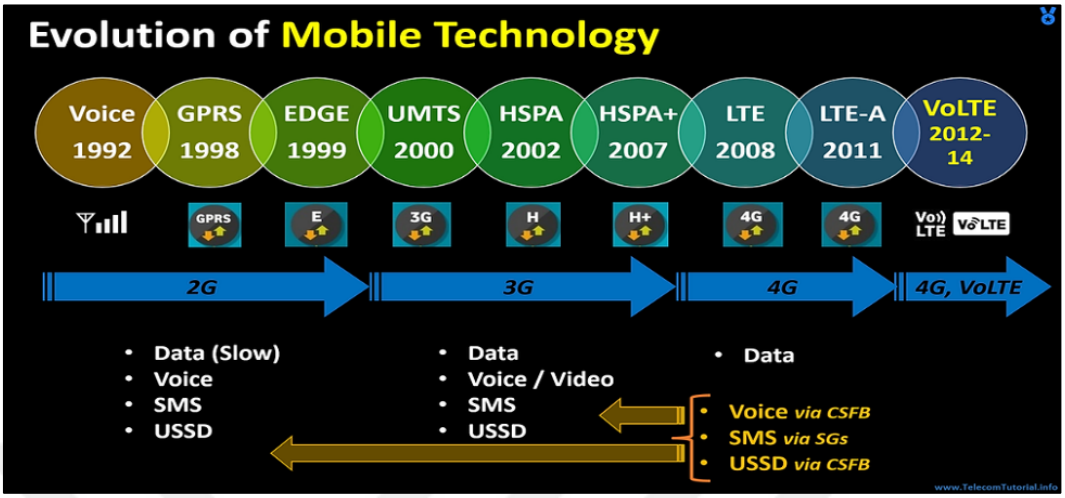

Figure 1.1: Evolution of Mobile Technology

In 2015, a conference was held by representatives of ITU who are responsible for the development of radio communications and set the vision of IMT 2020, and this is what is called today the fifth generation(5G) and a set of specifications that must be included in the system were identified, including low latency (URLLC), high reliability, advanced antenna tech. massive (MIMO),Millimeter waves (mm wave) , the Internet Of Things (IOT), spectrum flexibility, and among these organizations are Standard Development Organization (SDO) [2], The initial release 15 and release 16, as illustrated in figure below (Figure 1.2).

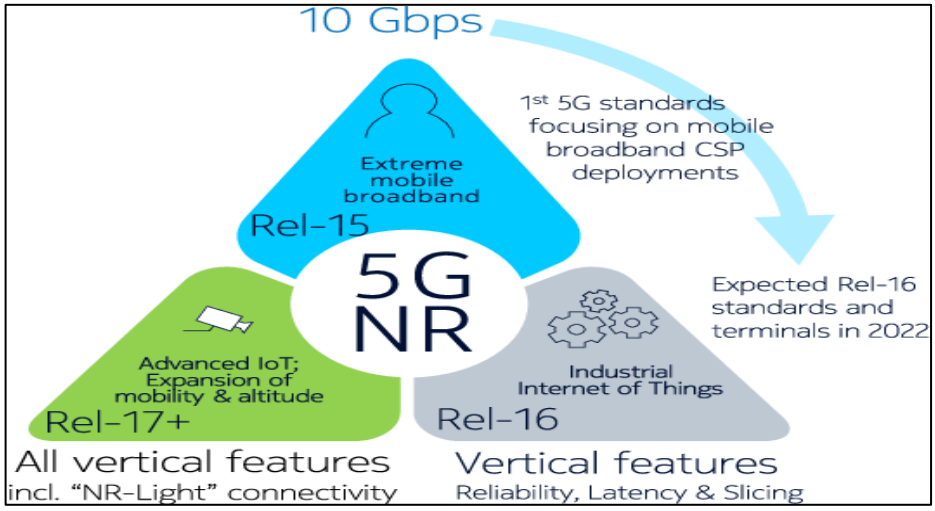

Figure 1.2: 5G development.

1.1 PROBLEM STATEMENT

MIMO systems are an important solution to the challenges of 5G networks that must meet many requirements, including high data rates, low latency, and high reliability. Traditional algorithms cannot handle many problems, but when investigating deep learning (DL) algorithms, it is appropriate to use these algorithms to solve them. When using deep learning, MIMO systems in wireless networks are optimized in terms of reducing computational complexity and improving power consumption. We present Rx-NN, a fully convolutional deep neural network. This Rx-NN neural receiver replaces hardware channel estimation, equalization and demodulation resulting in reduced complexity, in addition, eliminating these three devices leads to the possibility of reducing or not having to use the experimental signals used to improve channel estimation, From the signal stream in the frequency domain to the decoded bits, the complete receiver pipeline compatible with 5G networks is implemented, and we make accurate channel estimation possible by creating a convolutional neural input, using experimental data and code, and networking in a very special way. In addition, Rx-NN creates bits that are compliant with the 5G systems' use of channel coding. We show that Rx-NN outperforms traditional approaches use 3GPP-specific channel models. In addition, we illustrate a high-performance system that has been trained for the direct detection of uncorded bits from frequency domain antenna signals. Furthermore, Rx-NN has been trained to support various private 5G networks through experimental configurations and modification plans. The difficulty we encountered in connecting this neural receptor, the number of OFDM tokens should be equal to the number of nodes of the input layer of the Rx-NN when building the neural network so that both symbols. For the unknown and known convolutional input channels were generated using the experimental tokens. As a result, channel estimation using Rx-NN efficiently utilized experimental data and codes. Rx-NN outperforms traditional methods in terms of channel estimation and equalization by using simulation models to send uplink and downlink data in 5G, in fact, it shows how Rx-NN can effectively deal with non-Gaussian noise and interference. We demonstrate that larger performance gains can be obtained by carefully planning the architecture of the neural network and its inputs. According to our research, the majority of benefits are achieved by allowing the nervous system to use and distribute codes of

unknown data to improve the accuracy of channel estimation. By doing so, it enhances the radio performance of each device within the network. By approaching the implementation of the radio receiver as a supervised educational topic, it is feasible to take into account numerous individual receiver tasks, such as channel estimation and equalization, together. This work's main argument is that doing so will produce performance that is superior to optimizing each component separately. This type of technique has the benefit that the receiver's task can be characterized as a secondary educational challenge. The receiver's job is to extract information bits from an orthogonal frequency division multiplexing (OFDM) waveform that has been modified to match the waveform it has just received. without the need to apply manual classification methods or existing algorithms. Actually, the input data is simply the received waveform in the frequency domain, while the original transmitted bits are the corresponding labels. RxNN is able to perform all functions (channel estimation, equalizer, de-mapping removal) simultaneously because it has been taught to collect Log- likelihood ratio (LLRs) directly from the field antenna data frequency.

1.2 OBJECTIVES

The main goal of this project is to employ an OFDM channel model with a neural receiver dubbed Rx-NN that takes frequency selectivity and channel aging into account. This neural receiver replaces channel estimation, optimizer, and demodulation to reduce the computing complexity of those involved in optimizing wireless networks that use Massive (MIMO) systems. It does this by employing a small number of orthogonal pilots for channel estimation. An upgraded neural transceiver can consistently detect the code without the use of orthogonal pilots thanks to operation across multiple subcarriers and OFDM codes, which results in a considerably lower Bit Error Rate (BER). Gains in productivity are possible because no transmission-related renewable energy from bookmarks is lost.

1.3 FIFTH GENERATION COMMUNICATIONS

The term 5G refers to mobile networks with superior communication capabilities compared to other current networks, where there are three main scenarios for the use of this network, which are Enhanced Mobile Broadband (eMBB), which refers to the high rate of transmission and

reception of data such as virtual reality, augmented reality, games and video, which depends On the population density in urban and rural areas, mobility speed and network power quality [3], where the data transfer rate can reach (20 Gbps) and spectral efficiency up to (30GHz), as for the other scenario, which is mMTC, this describes how many devices are connected to the network with Low data transfer rate as the number of networked devices can reach up to one million devices per square kilometer, while URLLC covers scenarios that require low latency with high reliability such as self-driving cars and factory automation[4], the default distribution of system components unlike the concept of fixed components in Other systems is one of the most important features of the 5G system, where resources are allocated to these components according to the required service, which leads to an increase in the efficiency of the network in handling traffic, and this is called the concept of a slicing, which works with the three main scenarios of the 5G system, this is done by configuring chips inside the Base Station (BS) , which in turn serves a service for each type of service. The fifth-generation networks, commonly known as the New Radio (NR), employ a broad spectrum of frequencies beginning at SUB-6 GHZ. due to the rising complexity of wireless communication networks, and to attain millimeter wave (MM-wave) 60 GHZ, it has become necessary to use Artificial Intelligence (AI) techniques to manage these networks, which use millions of data and signals at every moment and for various fields such as the Internet Of Things (IOT), self-driving cars, automated factory management, medical fields, virtual reality and Augmented reality in addition to this, highlights the security concern for networks, with the increase in security threats, which have become difficult to address with old protection methods, artificial intelligence techniques enable the distribution and management of small cells used in 5G networks to save time, effort and cost, and also in systems Massive (MIMO) and Beam Forming (BF) to configure beams, direct the direction of the user and manage the huge amount of antennas used in the Base Stations (BS) of 5G networks. In 5G, mismatched services can operate in the same network architecture by network slicing technology [5], The principle of network slicing is due to network computing, communication, and storage resources. Radio Access Network (RAN), The RAN chips allocate the radio resources required for URLLC, eMBB and Mmtc devices in the time or frequency bands and consistent with the orthogonal assignment of wireless communications. Standard orthogonal, thus outperforming non-

orthogonal multiplexing (NOMA), which only shares radio resources between the same devices [6].

1.3.1 Enabling Technology Of 5G

The 5G wireless communication system can achieve the requirements through a set of technologies, the most important of these technologies, which enabled the system to reach this level of service.

1.3.1.1 Millimeter waves

They are waves with a frequency range between (30-300 GHz) that guarantees the general range and a wavelength of (1-10 mm), which is the reason for the name. These bands include (39 GHz, 37-42 GHz, 60 GHz) (figure 1.3), which in total provide a wide bandwidth A frequency range of (20 GHz), which is licensed bands, but the most widely used is the (60GHZ) band, which is currently used in industrial, research and medical applications, which are waves that provide a high data transfer rate [7]. Others broadcast in the form of concentric circles, and because they are waves of high frequency and short wavelength, they are not spread over many distances and are directed using radiation shaping techniques. These waves are also used to connect towers in the fifth-generation networks instead of wired connection, which provides high costs of connection between the constellations.

-

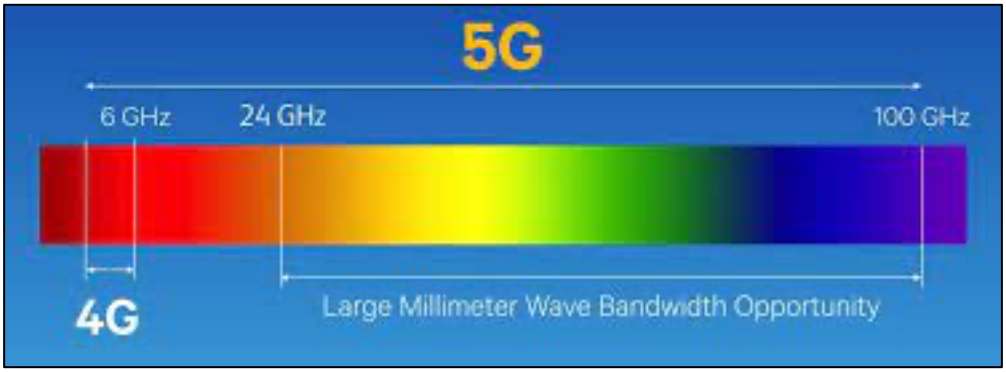

Figure 1.3: Millimeter Waves.

1.3.1.2 Beam-Forming

It is a method for concentrating the energy that antennas release in one direction while reducing the energy in other directions, which reduces the amount of signal interference needed for the user and over long distances. As figure below (Figure 1.4) shown the Beam-Forming of 5G, in the fifth-generation communication towers, there are hundreds of antennas in the base station (BS). These antennas contain arrays arranged in a geometric shape that allows transmitting and receiving signals depending on the sensing process, where the user is located. After the user service is completed the packet is routed to another user in the same way, and each array can send and receive multiple packets to a group of users and cover them. There are two types of stations in the fifth-generation towers which are the main stations and secondary stations. Transmitting and receiving between the two stations is done point-to-point and the secondary station covers users at long distances [8].

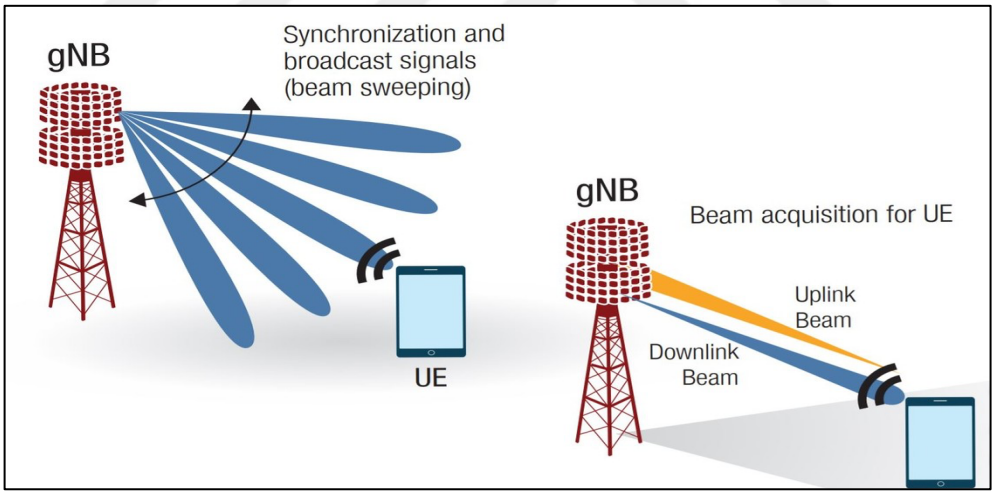

Figure 1.4: Beam Forming Technique.

1.3.1.3 Massive MIMO

One of the key innovations in 5G wireless communication networks, it entails the use of several antennas both during transmission and reception to improve the ability of devices to exchange data and correct faults., as we have hundreds of antennas in base stations (BS) compared to dozens in users' devices, which led to an increase in speed Network, increase network paths,

and increase network reliability [9]. In the fifth generation communications networks, these antennas are operated in a harmonious manner and are adapted, and the development of the MIMO system synchronously With the advancement of digital signal processing methods and the encouragement of concurrent user station scheduling, the link's reliability has improved thanks to spatial variety and increased energy efficiency, as the base stations check Broadcasting periodically to detect unwanted trends to reduce interference and improve access time and this is done using artificial intelligence techniques to estimate channel quality[10]. The main elements of the Massive MIMO system are pre-encoding, packet formation, encryption and detection, and the use of effective modern technologies to implement these elements It leads to reducing network complexity, improving detection and shortening training time the number of antennas has increased, and as a result, an increase in network capacity with high channel width, better power consumption rate, and reduced latency and the system shown in figure below (Figure 1.5).

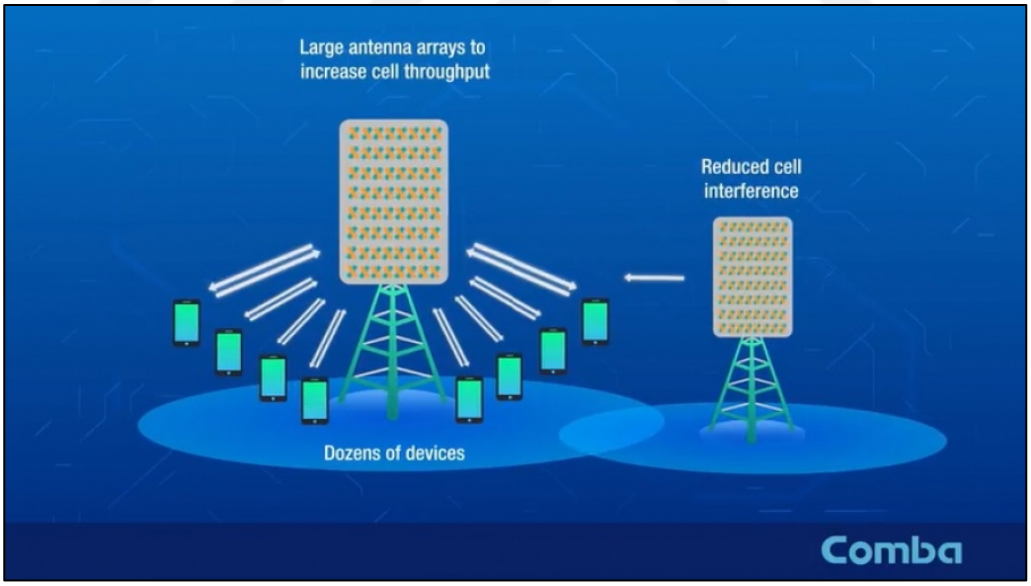

Figure 1.5: Massive MIMO.

1.3.1.4 Small cell

The increasing growth of cellular networks during the few years has led to an increase in data consumption rates for mobile phones, especially the fifth-generation networks. This increase

prompted service providers to develop infrastructure to accommodate this need to use data, which requires rethinking the use of large base stations covering a radius of a few miles It is not enough to cover or capacity for the enormous number of linked devices and the associated costs, so there was a need to use more small base stations, which are known as small cells and distributed antenna systems to help improve capacities and at increasing speeds up to (100 MHz per second). In some areas, these cells are characterized by a small target coverage area $<$ 10,000 ft^2) and have a low capacity with low power consumption ($<$ 30 w) and cover a limited number of users (up to 28 users) (Figure 1.6) [11]. With the advent of artificial intelligence techniques appeared what is known as Self-Organization Network (SON) cells that organize themselves without outside interference.

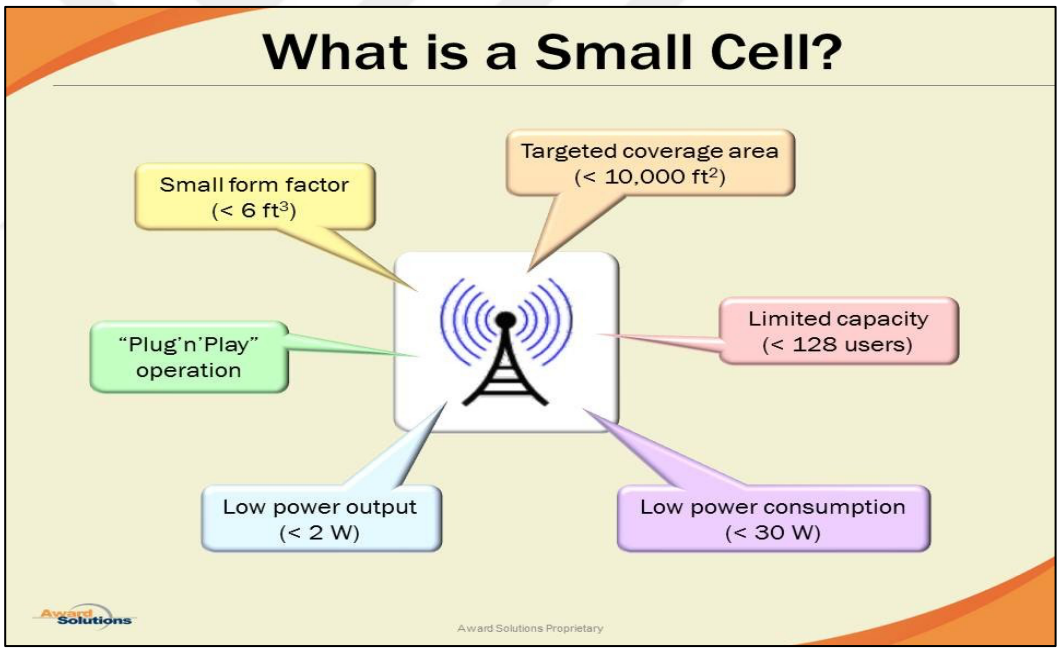

Figure 1.6: Small Cell.

1.3.1.5 Full duplex

Historically, full duplex communication is associated with the origins of human communication, and the telegraph can be considered the first application of two-way communication in the nineteenth century through the use of one or more pairs of telegraph cables to implement synchronous transmission. The best example of this type of

communication is phone calls, where all users of the call may simultaneously send and receive voice. In traditional networks, two separate channels were used to implement duplex transmission in both FDD and TDD. This causes a loss of part of the frequency spectrum, but in 5G networks. The same channel is used to implement duplex transmission, which improves network efficiency and reduces delays in peripheral devices [12]. The application of this technology faces more than one challenge, the most important of which is self-interference, and many techniques have been used to overcome this challenge and one of the most important These technologies are the antenna cancellation technology as well as the analog circuit technology.

There are two other types of transmission and reception, the first type is Simplex, in which the transmission takes place in one direction only, the second type is Half duplex, in which the transmission and reception takes place between two devices, the first one sends and the other receives only, and after the end of the transmission, the other device can transmit at another time, and the duplex types of systems as shown as in figure below (Figure 1.7).

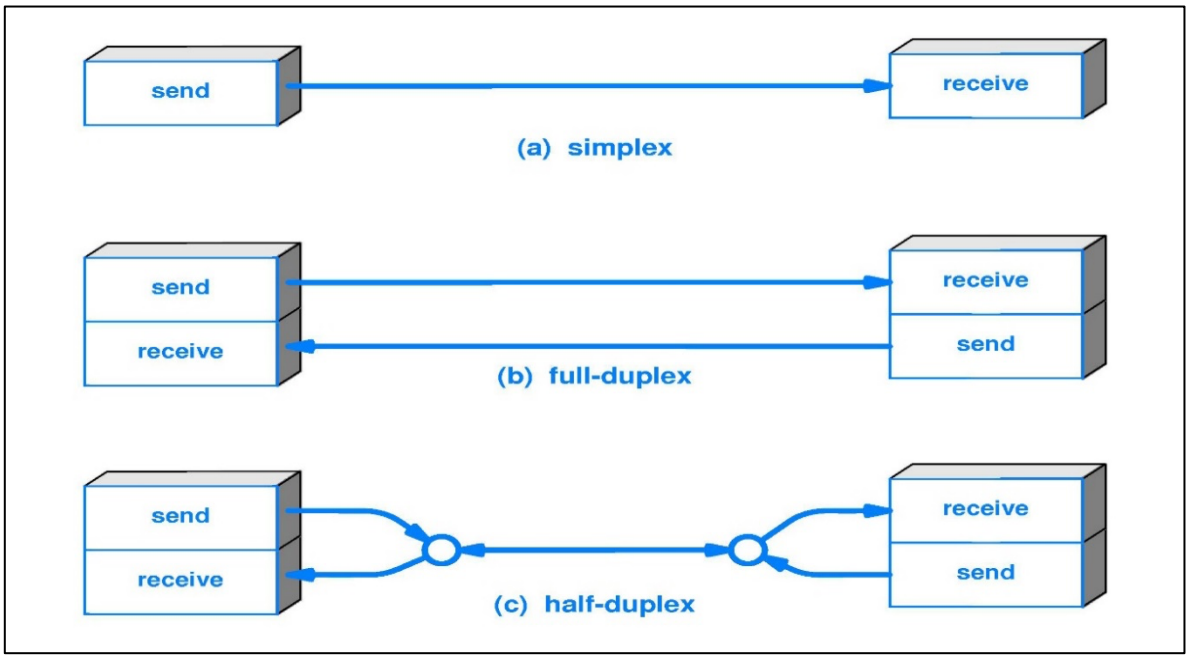

Figure 1.7: Duplex types of systems.

1.4 ARTIFICIAL INTELLIGENCE

When talking about the subject of artificial intelligence, it is necessary to address the first pioneer in the field of artificial intelligence (Alan Turing), who was a mathematician from Britain and had contributions the disciplines of mathematics, philosophy, cryptanalysis, and artificial intelligence,[13] and the paper he published is considered Alan Turing "Computational Machines and Intelligence" serves as the beginning to prove the intelligence of the machine, and he discussed the conditions necessary to consider the machine as intelligent, characterized by the speed of response, like the human being. The large computational led to a wide spread of artificial intelligence [14], and its application depends on the study of how the human mind thinks in order to solve the difficulties and issues it faces, arrive at the best solutions, and use those results as a benchmark for the creation of intelligent systems. (AI) has applications in voice and language translation, planning, natural language, expert systems, speech recognition, and robotics, scheduling and optimization as shown as in figure below (Figure 1.8). As well as artificial intelligence systems replace traditional systems that require the use of a lot of manual tuning [15]. At present, artificial intelligence is a very broad topic, where artificial intelligence techniques are combined with other technologies to obtain highly efficient systems.

Figure 1.8: Applications of AI.

In the field of wireless communication systems, many artificial intelligence algorithms, whether recurrent neural networks (RNN), have been investigated to meet the challenges of modern wireless networks and because of the challenges that these networks have to meet the unprecedented demands to reach a high rate of transmission and reception of data as well as record numbers. Because of the low response time, high degree of adaptability in resource management and design that characterizes the fifth generation wireless communications (5G) networks, giving them the high possibility to implement the requirements of users for these networks, the integration of Software-Defined Network (SDN) functions with Virtual Network Functions (NVF) led to Reaching the required flexibility, through which the system was allowed to modify itself in real time to implement traffic requirements, improve resource allocation, user mobility, and improve the system quality. And researching theories of artificial intelligence (AI) to provide the necessary flexibility and intelligence in the fifth generation (5G) networks. Encrypting strength, modulation, security, interference management, temporary storage, network segmentation, and improving energy efficiency. has led many research papers, surveys, and programs for learning how to use artificial intelligence in wireless communication networks.

1.4.1 Deep Learning

The definition of Deep Learning (DL) is an extension of traditional Machine Learning (ML), and the expansion is by adding more deep hidden layers (complexity) to the machine learning network layer model, and the data in these networks is represented hierarchically by some functions used to deal with Data and at multiple levels, Deep learning network (DL) layers may learn features from raw data and extract features from those features. Increase classification and prediction accuracy and reduce error in regression problems according to the topology used to build (DL) networks. Encoding and decoding systems, long-term memory networks, and activation functions. These types of deep learning networks have the ability to adapt to a range of highly complex challenges and achieve high technical outcomes. With the accuracy and accuracy of classification, Deep Science Network layers can handle different types of data such as bitmap (images and video), audio data, translation between natural languages, speech

recognition, as well as serial data**,** (Figure 1.9) shows the architecture of a full connection type convolutional neural network.

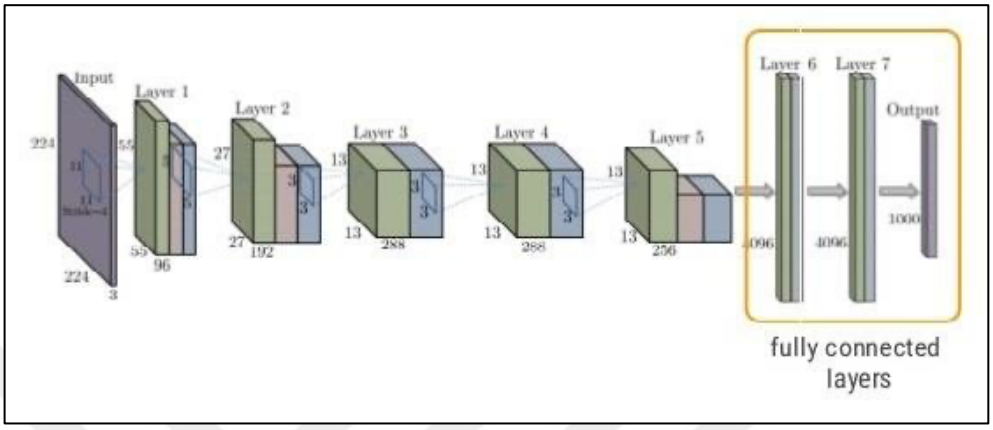

Figure 1.9: Caffe Net, an example CNN architecture.

One of the deep Recurrent Neural Network (RNN) models based on periodic feedback is Long-Term Memory Networks (LSTM). Traditional recurrent neural networks' training phase has two issues: gradient disappearance and gradient explosion. Long-Term Memory Networks (LSTM) fix both issues (RNN). (LSTM) consists of three types of gate structures, but with greater computational and time complexity. For this reason, the Gated Recurrent Unit (GRU) networks are used, which consist of only the update gate and the reset gate, which leads to eliminating the problem of computational and time complexity in (LSTM) and these gates in the structure of (GRU) networks give the ability to hold long-term states and remember them (Figure 1.10) illustrates a diagram of the (GRU) network.

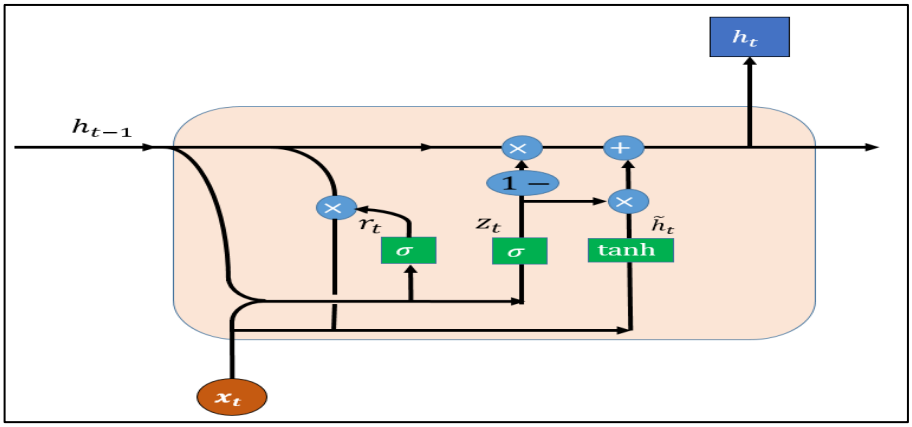

Figure 1.10: Structure of a GRU Cell.

1.5 RELATED WORK

In the next part, we will discuss some of the earlier research projects that used artificial intelligence methods, especially deep learning, to enhance efficiency and simplify wireless networks that employ MIMO (multiple input, multiple output) technology.

1.5.1 Hybrid BF Techniques

There are many traditional hybrid BF technologies, and we will illustrate three groups of these technologies: the hybrid technology based on the code book, the MIMO package space in the literature, and the scattered hybrid BF. The first type, the BF code book-based approach, is discussed and studied extensively in [16,17,18] because it combines complex structure with high quality. The major criterion for choosing Beams in this system is the greatest (SNR), which is in addition to interference [18]. MIMO system is used with one base station (BS) k, here there are NT antennas and LT (RF) chains in Base Station (BS) and at the end of User Equipment's (UE) there is only one antenna, even power distribution is assumed Among the users (UE) by the authors of [16], the signal received on the mobile user k is given as follows:

$$yk = h_k^T T_{RF} t_{BB}^k sk + \sum_{j \neq k}^{K} h_k^T T_{RF} t_{BB}^j sj + vj \tag{1.1}$$

where hk $\in$ C NT $\times$ 1 the channel vector, TRF $\in$ C NT $\times$ LT the RF precede, and TBB $=$ [t 1 BB, . . . , t K BB] $\in$ C LT $\times$ K the baseband pr-ecoder. Then, the received Signal to interfere Noise Ratio (SINR)at the (kth) user is denoted by :

$$\text{SINR}= \frac{P/h_k^T T_{RF} t_{BB}^k/2}{K\sigma_V^2 + P/h_k^T T_{RF} t_{BB}^k/2} \tag{1.2}$$

P represents the total transmission power while. represents σ_V^2 White Additive Gaussian Noise (AWGN). The RF and baseband primary encoders for mobile users are obtained by tackling the optimization problem, as in the following equation;

$$\{T_{RF}^* , \{T_{RF}^k \quad ^*\}_{k=1}^K\} = \arg\max \sum_{k=1}^{K} log_2 (1 + SINR_k) \tag{1.3}$$

$$s.t. \quad \left| T_{RFi.j} \right|^2 = \frac{1}{NT}$$

$$\| t_{BB}^{k} \|_2^2 = 1,$$

The $\mathbf{T}_{\mathbf{RF}}$ i, j represents the jth column element and the ith row element in the $\mathbf{T}_{RF}$ matrix. However, the hybrid BF based on the codebook is still complicated to search for the ideal configuration and compared to the array systems for large antennas is very high. In [16] advanced near-perfect codebook-based algorithms for hybrid RF are presented. In [17] depending on the supporting beams, we reduce the number of potential RF carriers, this depends on a number of variables, including the acting force and the direction of the Angle-of-Arrival (AoA), and then a full investigation is carried out in the small group that contains the beam converters. The authors of [18] propose to provide a feedback channel for the multi-user hybrid BF algorithm that has two phases that are low in complexity and also to find the best packet converters by reducing the search space on the packet offers available in the codebook, special suggestions for iterative algorithms are presented in [19], in [20] it is suggested that the estimation of the paths with a large dominance of the channel and the construction of the hybrid packet converters as a basis for designing the BF codebook, and by iterative search of the codebook, the parameters of each path are approximated in all stages of the algorithms, in [21] the authors suggest Packet aggregation techniques to get the best packets by utilizing Direction-of-Arrival (DoA) and direction-of-departure (DoD), In [22] the proposed algorithms are described as near-perfect. These semi-perfect algorithms use scattered approximation techniques containing different literatures that mixed between the hybrid (BF) and the scattered channel estimation technique in which the measurement matrices are the same as the hybrid beam converters and the channel estimation issue is A discrete estimation problem which is used by compression sensing-based algorithms to solve. In [23] the MM wave system which includes BS base station and L_T RF and NT chains per mobile user k, pre-training and vector combination, is searched in BS and kth the mobile user is presented as P_m and q_n and then user k is given the received signal:

$$\boldsymbol{y_{n,m}} = \boldsymbol{q_n^H H_k p_m s_m + q_n^H n_{n,m}} \tag{1.4}$$

where $H_k \in C\ NR \times NT$ channel matrix between the (BS) and the kth user and s_m the precoding vector contains the training symbol P_m , In the training phase, the average power used per transmission is set to P, and It's believed that s_m = √ P. 36 , the received signal matrix is defined as:

$$\mathbf{Y} = \sqrt{\boldsymbol{PQ}^*}\boldsymbol{H_k p} + \boldsymbol{N}, \tag{1.5}$$

where **Q** = [q_1, ..., q_{Nr}] and P = [p_1 , ..., p_{Nr}] are the measurement matrices. N is an N_R × N_T noise matrix. The authors of [23] then victories the received signal matrix Y to take use of the channel's sparseness as:

$$\mathbf{Y}=\sqrt{\boldsymbol{P}}\ (\boldsymbol{P^T}\otimes\boldsymbol{Q}^*)(\boldsymbol{a}_{\boldsymbol{T}}^*(\boldsymbol{\phi_k})\otimes\boldsymbol{a_R}(\boldsymbol{\theta_k})\boldsymbol{\alpha_k} + \boldsymbol{v}, \tag{1.6}$$

where $\boldsymbol{\alpha_k}$ is the complex path gain, a_T ($\boldsymbol{\phi_k}$) and a_T ($\boldsymbol{\theta_k}$) are the BS and kth mobile user's antenna array response vectors , respectively. Moreover, (AoDs) and (AoAs) are taken from a grid of N and M points, respectively. Then, y in (1. 5) is approximated as,

$$\mathbf{Y}=\sqrt{\boldsymbol{P}}\ (\boldsymbol{P^T}\otimes\boldsymbol{Q}^*)\ (\boldsymbol{A_T}\otimes\boldsymbol{A_R}\ )\boldsymbol{Z_k} +\mathbf{v}, \tag{1.7}$$

Initially the P-training pre-configuration matrix is built at the base station of $[P]_{i,j} = e^{j\emptyset i,j}$where $j\emptyset i,j$ is taken by random quantitative angles $\{0, \frac{2\pi}{N_Q^T}, \ldots, \frac{(N_Q^T-1)2\pi}{N_Q^T}\}$.

N_T × N matrix A_T^- and N_R× M matrix A_R^- representing the dictionary matrices, N_Q^T representing the building blocks, the Q matrix that collects the training built by each mobile user and then each entry $\Phi = P^T \otimes Q^*$is set to e^{jy} is assigned to Q by taking models Samples from angle Y randomly from a quantum package, and by recovering the ZK scattered vector support by OMP the user guesses the mobile phone kth AOD, AOA for his channel and independent to the following equation :

$$\boldsymbol{support}\ (\boldsymbol{Z_k}) = \ \mathbf{arg\,max}\ \boldsymbol{\Phi}^*\ \boldsymbol{\Psi}^*\boldsymbol{y}, \tag{1.8}$$

where $\Psi = A_T^* \otimes A_R$. Then, the AoD $\hat{\theta_k}$and the AoA $\hat{\phi_k}$ are estimated by using support (Z_k). The RF combining vector of the kth mobile user $\boldsymbol{r_k}$ in [23] is designed as $r_k = a_R(\hat{\theta_K})$. After each mobile station sends the index of its estimated AoD to the BS, the BS computes its RF precoding matrix as $T = [\, a_T(\hat{\phi_1}), \ldots\ldots, a_T(\hat{\phi_K})\,]$. Hybrid BF for multi-user massive (MIMO) systems using WMSE sum-squaring error and according to the algorithms suggested by the authors of [24].

1.5.2 Wireless Networks with Massive MIMO

Number of antennae growing being used in base stations (BSs) is directly proportional to the high possibility of increasing the data flows through the network. This increase in the data transfer rate is accompanied by an increase in the reliability of communication by spatial diversity, which leads to a reduction in energy emission and a high efficiency of the network away from The system's complexity and the quantity of measurements, and because the Massive (MIMO) system has the possibility of wide freedom and greater selectivity in the process of sending and receiving data with a high possibility of canceling interference, the Massive (MIMO) system also provides a network with latency by avoiding transmissions in the directions that are not required by the base stations (BSs). Combining Massive (MIMO) with beamforming (BF) techniques, this procedure enhances the signal-to-noise ratio (SNR) while smoothing out vanishing droplets [25]. The authors present in [26] an important matter which is the relationship between the large correlation between number of antennae used in and between the higher improvement of the channel estimation quality for each antenna and the increased response. The high routing of the signal in the right place and the lack of interference to multiple users by using the Massive (MIMO) A major boost in network capacity, energy efficiency, and maintaining a low rate of heat emission was made thanks to multi-spatial systems [27]. The authors of [28] presents the view of the participation of all users in the multiplexing gain. Therefore, the antenna array deployment process is done in the base stations (BS) only to reduce the costs resulting from the deployment of these antennas in the base stations (BSs). Participation and providing more complications for used equipment and lower costs in addition to preventing interference and reducing the impact of noise and fading. In [29]

the authors suggested the literature for cooperative or non-cooperative massive MIMO systems where all BS serve a specific user and are called networked mega-MIMO systems. These connected BSs have relatively few antennas, the communication between these base stations is data and Channel Status Information (CSI) shared by downlink (D-Link). The data is flowed in a participatory form from BS using Beam-Forming (BF) technology at some times, which often leads to the prevention of interference cases. The authors of [30] focused in their study the challenge based on Channel Status Information (CSI) feedback in massive MIMO systems, especially the use of spatial-temporal correlation to reduce the feedback burden and to reach an accurate estimation of the channel state by transforming the coherent (CSI) into a sparse vector. It is not connected in some base stations by means of pressure sensing (CS) and on the basis of this principle, protocols were developed for reactions (CSI) and many advanced algorithms were presented, but these algorithms face many challenges, including that (CS) algorithms are slow in Reconstruction of iterative signals, as well as the assumption based on widely scattered channels in the rules, and these channels may not be scattered in the first place, in addition, the random projection of (CS) algorithms does not absorb the channel structures sufficiently, for this reason, artificial intelligence (AI) techniques and Especially Deep Learning (DL) in the face of these challenges. In [31] proposes an approach based on deep learning (DL) methods in massive MIMO to encode Channel State Information (CSI), deep learning (DL) which is used to perform a specific task by inserting large samples into the network to train multiple neural layers. Layers, initially used for deep learning (DL) in the reconstruction of natural images and has achieved great success in this field, which led to its use in the reconstruction of wireless channels, despite the fact that reconstruction of wireless channels is more complex or difficult than reconstruction Natural images, but experiments also showed success in the (CSI) recovery process with high quality and improved by using one of the types of deep learning networks (DL), which is the sensor network (encryption) and recovery (decryption), which is called (CsiNet). Through training data, this network learns to transition from the original channel matrix to condense representations and utilize the channel structure effectively, eliminating the random drop approach used in the prior conventional methods of coding. On the other hand, (CsiNet) network Reverse conversion and recovery of original channel arrays from encrypted words, avoiding redundancy (recursive algorithms) using a decoder, and returning code-words

to the base station. Since mm-Wave MIMO systems need a radio frequency (RF) chain for each antenna, the study in [32] focuses on the methods used to reduce the complexity of radio frequencies. However, because each antenna in these systems requires an RF chain, this procedure results in a significant energy consumption, high device costs, and an increase in the energy emitted by the many antennas used in Massive MIMO systems. Due to these factors, the study proposes two methods—the lens array-based hybrid pre-coding technique (LAHP) and the phased array-based hybrid pre-coding technique—to lessen the complexity of radio frequencies while converting from microwave to millimeter frequencies (PAHP). On the data transmission side, the process of selecting the (LAHP) network is done on the basis of low energy consumption and at a lower cost by traditional packets for channel estimation, while we use the retrieval problem of the scattered signal in the process of estimating the packet space, as well as the comparison between the efficiency of the two technologies about energy effectiveness and high capacity On the treatment of interference between cells and the percentage of error in estimating channel information and conditions.

1.5.3 Artificial Intelligence for Wireless Communications

The authors of [33] present the various techniques used to collect channel information, including the experimental channel estimation of the MIMO multiplex system, where one of the real data carriers sends sequences of experimental signals that are predetermined and then the highest probability is taken by Machine Learning techniques (ML) and that Estimating the channel states by determining the values that increase the probability of the previously sent indices relative to the received symbols by adopting one of using techniques like the Minimum Mean Square Error (MMSE), It lowers the average error between the channel coefficient matrix's real and estimated values, as for the Least Squares method (LS) It reduces the squared distance between the experimental symbols vector and between the received symbols vector, and these methods are considered the most popular. The authors of [34] present proposals in wireless communication systems in which artificial intelligence (AI) algorithms are used in dealing with high data traffic and in various scenarios, which are characterized by being less computational complexity than traditional algorithms while maintaining high performance rates for those systems, achieving The authors in [35] in the approaches presented by artificial

intelligence (AI) techniques to help find appropriate solutions to the challenges facing the application of modern communication systems such as (channel estimation (CS), massive MIMO communication systems, millimeter waves MM wave), channel state information (CSI), beam-forming (BF) , additionally, the Non-Orthogonal Multiple Access proposal (NOMA) schemes in conjunction with long-term memory (LSTM) to determine channel characteristics, in addition to the use of deep learning techniques (DL) by DNNs along with massive MIMO systems for direction of arrival (DoA) and channel estimation and provide a comprehensive review of all solutions offered based on the deep learning literature (DL) of its various types to help develop scenarios for the fifth generation of communications (5G), especially with the great successes of (AI) technologies and algorithms in other fields. In the literature [36] in the narrow beamforming (BF) system, a massive MIMO system with millimeter wave (MM wave) is proposed based on deep learning (DL) algorithms, where the geometric mean analysis (GMD) method is adopted to perform the auto-encoding process for digital devices and on the other hand, the paper presents a schematic for a narrow beamforming (BF) system. This scheme performs diversified transmission with relation to the state of the channel or on the spatial multicast and depending on the method of link conditioning and by machine learning algorithms (ML) and in all methods that depend on Deep learning (DL) datasets that are trained to select packets are built in various systems scenarios (MM wave and massive MIMO). In addition, in the process of estimating digital and analog encoders based on the different channel states of the BF system, DNNs are trained with the parameters resulting from those states of the channel. In [37] a proposal was made to reduce the number of radio (RF) chains through a beam space channel model based on lens antenna array, but the big challenge in massive MIMO systems and The support detection (SD) method is used to prepare the channel estimation scheme, in the massive MIMO system when we have a limited number of radio chains and a large antenna array, which results in the inability of the received signal matrix from the lens antenna array to focus and scatter the energy. This approach breaks the channel estimation challenge down into a number of smaller issues , and in another study in The beginning is the creation of the channel matrix, then using the (SCAMPI) algorithm, which provides two-dimensional (2D) natural images, then the approximate analysis of the algorithm derived from the image retrieval method and the use of the(EM) prediction maximization algorithm to gather Gaussian mixture (GM)

parameters from the current data and consider the Massage – Passing - interface (SCAMPI) algorithm as a distributor General probability of a Gaussian Mixture (GM) ,In this study, the Saleh-Valenzuela channel is relied on in the wireless communication model of mm-Wave systems, and the packet space channel matrix is expressed by the following equation:

$$M = \sqrt{\frac{MN}{P+1}} \sum_{i=1}^{P} \propto^{i} A(\varphi^{i}, \theta^{i}), \quad (1.9)$$

$H \in R^{N*M}$ represents the beam space channel matrix, $P + 1$ the number of paths. The term $\propto^{i}$ represents the path gain and the values φ^{i} and θ^{i} refer to the height and azimuth (AoAs) of the incoming waves and the antenna array response matrix By $A(\varphi^{i}, \theta^{i})$, for signal recovery, estimating the massive MIMO beam space channel is a typical issue. Initially, by routing H to rest, the beam space channel vector $h \in R^{MN*1}$ is obtained in the uplink training phase. , at the base station (BS) the user sends the training code to the base station (BS) and the user is given the received signal vector $y \in R^{MN*`}$

$$y = hs + n, \quad (1.10)$$

where $n \sim N(0, \sigma \propto_n^2 I)$ represents a vector of Gaussian noise. Given a receiver choice network W, the received signal r from the RF chain can be represented as:

$$r = Wy = Wh + n^{-}, \quad (1.11)$$

After the process of determining the network at the receiver, $n^{-} = Wn$ represents the equivalent noise that is dependent on $\boldsymbol{N}(\mathbf{0}, \boldsymbol{\sigma} \propto_{\boldsymbol{n}}^{\mathbf{2}} \boldsymbol{I})$, each element in the array **W** is normalized by dividing $\sqrt{\boldsymbol{MN}}$, and the antenna array response matrix links the components of the undeceived beam space channel vector, and it can be applied the Learned De-noising-Based Approximate Message Passing (LDAMP) network resulting from the recovery of natural images, because this method is very similar to two-dimensional (2D) natural images, in the sense that the channel is scattered and the variations between nearby elements in the matrix are very accurate, and thus exploiting the correlation in estimating the beam space channel. The ***L*** neural layers that make up the (LDAMP) network are connected in series and these neural layers

share the same structure. Each layer contains the same slider $D\sigma\hat{}l(\cdot)$,and the same divergence estimator $vD\sigma\hat{}l(\cdot)$, and the weights used. (DnCNN) is used to update $\boldsymbol{h}$ and it is estimated.

$$Z^{l+1} = r - Wh\hat{}^{l+1}\frac{1}{k}Z^{L}\, divD\sigma\hat{}l(\, h^{l} + W^{T}\, z^{l}) \tag{1.12}$$

$$h\hat{}^{L+1} = D_{\sigma^{l}}(\, h^{l} + W^{T}\, z^{l}) \tag{1.13}$$

where $h\hat{}^{L}$ is the $l-th$ input layer for the channel, Z^{l} displays the$l-th$ layers of the residual vector's input, and $\sigma\hat{}^{l}$ indicates a denoiser parameter, which is described as $\boldsymbol{\sigma\hat{}^{l}} = \| \boldsymbol{z^{l}} \| \boldsymbol{2\sqrt{K}.}$ If we consider the denoiser's contribution, $\boldsymbol{X^{l}} = \boldsymbol{h\hat{}^{l}} + \boldsymbol{W^{T}}\, \boldsymbol{Z^{l}}$ as a noisy channel vector:

$$X^{L} = h + \mathrm{n}\hat{}^{l} \tag{1.14}$$

And the equivalent noise $\mathrm{n}\hat{}^{l} = h\hat{}^{l} - \mathrm{h} + \mathrm{W}^{T}\,\mathrm{z}^{l} \sim \mathrm{N}\,(0, (\sigma^{l})^{2}\mathrm{I})$.The process of estimating the channel $\boldsymbol{h}$ on the part of the denoiser $D_{\sigma^{l}}(\cdot)$ by eliminating the noise equation $n\hat{}^{l}$ from the noisy channel X^{l} The estimated value of the Z^{l} vector is what determines the equivalent noise variance rate $(\sigma^{l})^{2}$ This eventually declines as the number of layers increases continuously, and convergence takes place Moreover, by Z^{l} eliminating the bias in the median solutions, $divD\sigma\hat{}^{l}(h^{l} + \mathrm{W}^{T}\,\mathrm{z}^{l})/K$ and then the model image reducers approximate then$\hat{}^{l}$ the following Monte Carlo approximation, equivalent noise values to the additive white Gaussian noise (AWGN) values is used to calculate the difference for that Due to the difficulty of obtaining an accurate expression for $divD\sigma\hat{}^{l}(\cdot)$ we give the slider $D_{\sigma^{l}}(\cdot)$ and using an independent random vector$b \sim (0, I)$ and use the following equation to estimate the divergence.

$$divD\sigma\hat{}^{l} = \lim_{\epsilon\to 0} E_{b}\{\, b^{T}\left(\frac{D_{\sigma^{l}}(X^{l}+\epsilon b) - D_{\sigma^{l}}(X^{l})}{\epsilon}\right)\} \tag{1.15}$$

In (LDAMP) networks, channel estimation is highly dependent on the splitter. Compared with other techniques, the (DnCNN) eliminator is faster and more accurate due to its high ability to deal with the problem of reducing Gaussian noise. The network layer structure plays a major

role in the network being very accurate and also reduces the Training times. In [38] the authors propose to integrate machine learning applications into modern wireless communication systems to perform the process of specifying the modulation grooves and coding through parenthetical learning classification and using Support Vector Machines (SVM).), that the optimization processes on the network in this literature differ from the traditional methods, but the optimization is done by generating data (codes) by continuously developing the model through training for long periods of multiplex-multiple-receive (MIMO) communication systems for spatial diversity by integrating deep learning techniques And the automatic encoders through a neural network (NN) trained to learn the bananas sent through the Rayleigh channel, and the process of estimating the symbols is done with high accuracy by removing the interference in the receiver, as the encoder learns the conditions of the channel (CSI) synchronously with the transmitted symbols. The production of the 5G of mobile systems (5G) is gradually meeting the requirements of more stringent end-user applications [39], [40]. It is challenging to monitor and manage data for many network parts due to the growing diversity and complexity of the mobile network. Thus, integrating flexible machine intelligence into future mobile networks is a subject of unmatched scientific interest [41]. This trend is reflected in the creation of Network systems that support machine learning techniques, as well as the use of machine learning (ML)-based solutions to issues ranging from malware detection to Radio Access Technology (RAT) selection [44], [45]. Systematic information value extraction from traffic data is made possible by ML, as is the automatic detection of links that would otherwise be too difficult for human experts to identify [46]. Deep learning, a machine learning pioneer, has demonstrated excellent performance in fields including computer vision [47] and Natural Language Processing (NLP) [48]. Researchers working in networks are also starting to understand the value and potential of deep learning and are investigating how it might be used to address difficulties unique to mobile devices. Field of networking [49], [50]. It makes sense to integrate deep learning into 5G wireless networks and mobile networks. Particularly, because they are frequently gathered from various sources and in various forms, the data produced by mobile settings are becoming more and more heterogeneous. In contrast, because big data uses hierarchical feature extraction as opposed to domain knowledge, it enhances the performance of deep learning. In essence, this means that data may be incrementally abstracted, and

information can be efficiently extracted while requiring less preprocessing. Deep learning can draw inferences in milliseconds thanks to GPU-based parallel computation. Due to the removal of run-time constraints, high-accuracy and speedy network analysis and management are now possible, beyond the limitations of conventional mathematical techniques (such as convex optimization, game theory, and meta-inference).

1.5.4 Neural Network

Chang et al. in [51] apply convolutional neural networks (CNNs) to equalization, producing a smaller error vector magnitude than multi-modulus algorithm- or recursive least squares-based methods. Deep learning-based de-mapping is examined in [52]. where Shental and Hoydis recommend utilizing deep neural networks to effectively calculate bits. (LLRs) of equalized symbols are log-likelihood ratios. The proposed de-mapper is based on deep learning. is shown to achieve precision that is comparable to that of the ideal log maximum a-posteriori rule, but at a far reduced computing cost. Additionally, numerous articles recommend integrating deep learning components into the standard receiver processing flow. As long as the prerequisites are satisfied, [53]– [54], each of them surpassing the conventional receiver benchmark Training is carried out. Some academics have also considered the potential of building larger receiver parts with just one neural network. For instance, Ye et al [55].'s study of coupled channel estimation and signal identification makes use of deep learning. A fully connected neural network processes the data signal and the pilots there before doing the detection. This type of completely trained receiver is shown to function noticeably better than a normal receiver based on minimal mean square error when there aren't many channel estimate pilots or when the Cyclic Prefix (CP) isn't present (MMSE). In contrast, a receiver is constructed in [56] that calculates bit estimates directly from a time-domain RX signal, displaying exceptional performance at low to medium SNRs. The CNN-based method outperforms a linear least squares-based receiver even while it lags behind an MMSE-based receiver and a receiver with perfect channel information at high SNRs. Deep learning-based end-to-end systems, in which the transmitter and receiver are simultaneously learned from the data without any pre-specified modulation scheme or waveform, have also been thoroughly examined [57]– [58]. The capacity

of these methods to outperform traditional heuristic radio connections has been established, for instance by acquiring a better constellation shape.

1.5.5 End-To-End System

End-to-end learning has drawn a lot of interest recently and is seen to hold promise as a technology for future wireless communication systems [59], [60]. A single auto-encoder Neural Network (NN), trained to maximize information rate, is used as the transmitter, channel, and receiver in this system [61, 62]. Since its introduction in wireless communications [63], End-to-End learning has been used in various fields, including optical wireless [64] and optical fiber [65]. However, the majority of the research is either experimental but done in static settings [66] or simulation-based and uses simple channel models like Rayleigh block fading or additive white Gaussian noise (AWGN) (RBF). Comprehensive learning across OFDM channels is initially taken into consideration in [67]. The receiver is unable to benefit from the rhythmic spectral correlation of the OFDM channel due to the autoencoder's restriction to operating across individual Res, this approach is broadened in [68] to incorporate the PAPR technique's instruction. [69] co-optimizes the primary decoder and the decoder while taking into consideration one-bit quantization of the received OFDM signal in order to make it easier to reconstruct the broadcast signal. Recent years have seen relatively little focus on OFDM systems' neural receiver. The remaining convolutional NN is taken in [70], a convolutional NN that operates over a substantial number of subcarriers and OFDM symbols. Bit error rates (BER) in realistic 3GPP channel models are comparable to those possible with complete channel information. Additionally, it has been demonstrated that this neuronal receptor is more resistant to interference than traditional methods. The authors created a thorough teaching strategy in [71]. shared source and channel coding architecture without the need for pilots. On this subject, there is a wealth of literature that contains several systems that typically call for sophisticated detection algorithms.

2. MATERIALS AND METHODS

Wireless communications are considered one of the basic components of modern life and this type of communications has witnessed a great development in recent times, many researches and studies have been submitted to develop wireless communications systems in the field of increasing data transmission rates and ways to reduce energy consumption rates and address anomalies in wireless communication systems. Using a neural receiver that has been trained to take the place of the channel estimation, equalizer, and mapping removal in accordance with the system model diagram, we will create a communication system based on a multiple-input and multiple-output (MIMO) communication system to send and receive data between a user equipment (UE) and a base station (BS) for both Uplink (UL) and Downlink (DL).

As the figure following (Figure 2.1) is an explanation of the most important components of the system model.

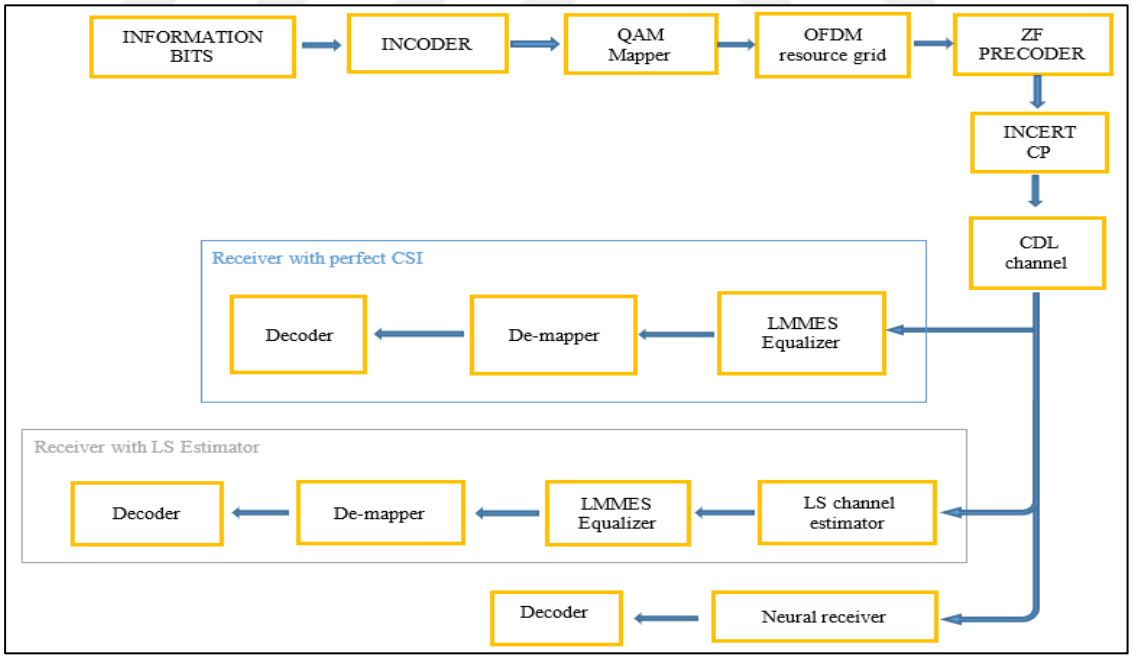

Figure 2.1: A graphical representation of the system model showing each necessary component.

2.1 CODING

In the presented system model encoding and decoding are done by Low Density Parity Chick

(LDPC), which was first introduced by the scientist R.GALLAGER in the sixties of the last century and was rediscovered by MACKAY&NEAL in 1996, and this method is considered the preferred method in performing the encoding and decoding process In modern wireless communication systems, because of its parallel implementation characteristics and good error correction performance, LDPC codes are the most used in Forward Correction Codes (FEC), as well as its codes served as a basis for modern coding theory, due to its dependence mainly on the SHANON theory [72] In broadband communications with high data rate, LDPC offers promising solutions. For the fifth generation of wireless communication technologies, the Third Generation Partnership Project (3GPP) established two base graph matrices (BG1) and (BG2) to facilitate scalable data transmission (5G), (LDPC) was used in the channel error correction schemes through (QC-NR-LDPC) symbols. (Figure 2.2) shows the basic structure of the (QC-NR-LDPC) structure.

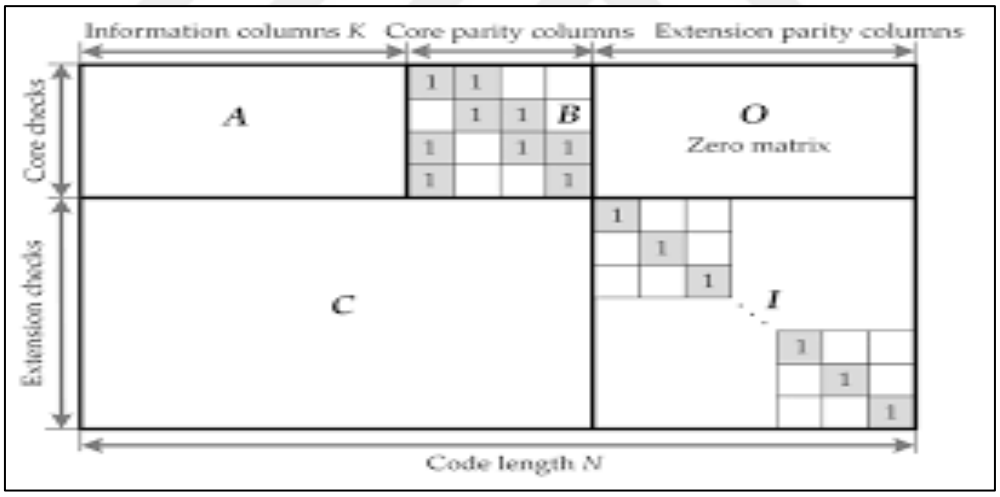

Figure 2.2: Drawing of the Quasi-Cyclic (QC-LDPC) codes.

Iterative decoding of (LDPC)method is strong in encoding noisy channels with high fading, and the difficulty in its application lies in the problem of how to merge the detector and modulator files with the code. This difficulty is dealt with by assigning the random LDPC encoded bits directly. On the modulated signals, design the LDPC code by arranging the maps in the receiver [73]. Consider LDPC code with length n and design rate $R = K/n$. This symbol's iterative decoder can be shown as a graph. It has checking nodes $K - n$, edge interleaves, and variable nodes. The number bit in the cipher is represented by the ith variable node. A bit participates

in $d_v^{(i)}$the parity check, then its node The edge$d_v^{(i)}$ enters the edge interleaving. Edge interleaving Connect variable nodes to validate nodes, each validation node It represents the equivalence check equation. Check ith the check $d_c^{(i)}$ node So bits have $d_c^{(i)}$edges. Variables and check groups. The nodes are called Variable Node Decoders (VNDs) as well as Check Node Decoder (CND). Repeated action decodes by using message relaying between VND and CND, it is put into practice. The decoder's architecture is shown in (Figure 2.3).

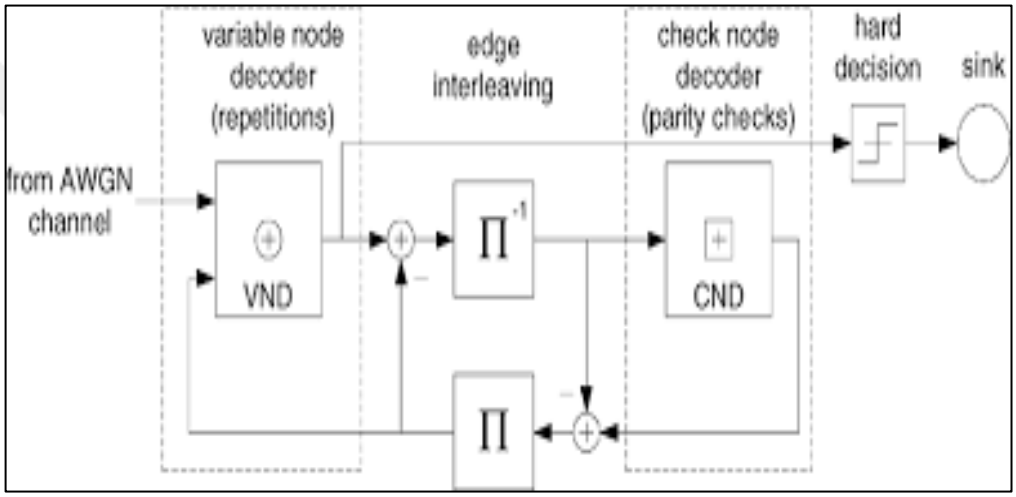

Figure 2.3: An LDPC code iterative decoder

based on a combination of external single parity codes and internal duplicate code. this insight explains how LDPC decoding and other iterative decoding techniques, such B. Turbo decoding, are closely related [74].

2.2 MODULATION

In electronics, the technique of imprinting information (voice, music, images, or data) on a radio frequency carrier by changing one or more properties of the wave in response to the information signal. There are different forms of modulation, each designed to alter specific characteristics of the carrier. The most frequently changed properties include amplitude, frequency, phase, pulse rate, and pulse width. Modulation, in electronics, the technique of leaving information (speech, music, images, data) on a radio frequency carrier by changing one or more properties of a wave in response to an information signal. There are different forms of modulation, each

designed to alter specific characteristics of the carrier. The most frequently modified properties include amplitude, frequency, phase, pulse rate, and pulse width. Modulation, in electronics, is the method of printing information (sound, music, images, or data) on a radio frequency carrier by changing one or more wave properties in response to an information signal. There are different forms of preform, each designed to alter certain characteristics of the carrier. Frequently changed properties include amplitude, frequency, phase, pulse rate, and pulse width. Modulation, in electronics, is the method of leaving information (speech, music, images, or data) on a radio frequency carrier by changing one or more wave properties in response to an information signal. There are different forms of preform, each designed to alter certain characteristics of the carrier. Frequently modified properties include amplitude, frequency, phase, pulse rate and pulse width, in this model, Quadrature Amplitude Modulation (QAM) will be used. It can be applied to many formats: Although there are performance differences and trade-offs between 8QAM, 16QAM, 64QAM, 128QAM, 256QAM, QAM or quadrature amplitude modulation, it does provide some notable benefits for data transfer. SNR suffers when data rates increase from 16QAM to 64QAM, from 64QAM to 256QAM, etc. Many data transmission systems switch between QAM, 16QAM, 32QAM, and other QAM commands [75], depending on the state of the link, higher data rates can be exchanged to improve flexibility and reduce Bit Error Rates (BER). Including various forms of wireless communication, mobile communication, and the like.

Figure 2.4: Mapping the Bit Order for a 16QAM signal.

When there is sufficient headroom, higher order QAMs can be utilized to achieve faster data rates, however lower orders are employed when the link deteriorates to retain noise margin and

guarantee low bit error rates. As the QAM order increases, the distance between distinct locations in the constellation diagram gets closer, and the likelihood of introducing data mistakes rises. Employing higher order QAM forms requires exceptionally low Eb/No data mistakes for the link. In order to maintain the bit error rate as Eb/No declines, the power level must be increased or the QAM order must be decreased. Therefore, performance, an acceptable bit error rate, and data rate and QAM modulation order must all be balanced. Although more error correction can be done to prevent network degradation, it also slows down data transmission, in numerous radio communication, wireless communication, and mobile communication systems, QAM is used. But certain QAM variations are employed for certain standards and applications. The (SNR) and data throughput need to be balanced. The amount of data that can be transmitted under ideal conditions increases as the QAM signal order rises, e. g. from 16QAM to 64QAM, etc. The disadvantage of this is that it demands a higher signal-to-noise ratio. Although the order of the modulation formats is fixed on some platforms, bidirectional links on other systems allow the modulation order to be varied to increase throughput for a given link state. The level of error correction has also changed. By altering the modulation sequence and error correction, the data speed can be changed while maintaining the desired error rate. In digital cable TV and cable modem applications for domestic broadcasting, 64 QAM and 256 QAM are frequently used. Because transmission is only one-way, the QAM modulation order must be set at the transmitter, and there are thousands of other applications where using a dynamic adaptive modulation form of receiver is not feasible. The order of QAM modulation and error correction can be dynamically adjusted depending on the link between the two ends for many types of wireless and cellular technologies. The complexity of network adaption approaches increases as data rates and spectral efficiency requirements climb. To enable the connection to quickly adjust to the current connection quality and provide optimal data throughput, transmit power balancing, QAM ordering, forward error correction, etc., the data channel is carried over the cellular signal. The complexity of network adaption approaches increases as data rates and spectral efficiency requirements climb. To enable the connection to quickly adjust to the current connection quality and provide optimal data throughput, transmit power balancing, QAM ordering, forward error correction, etc., the data channel is carried over the cellular signal. The position of the QAM states, squared of the modulation amplitude, are

displayed in the constellation diagram. There are more points in the 16QAM constellation the higher the modulation order. The vertical axis is made up of square or "Q" elements, and the horizontal axis is made up of in-phase or "I" elements. I have a few posts to make. H. a particular pairing of I and Q for various data symbols. The 16QAM modulation format is depicted in the following figure below (Figure 2.5).

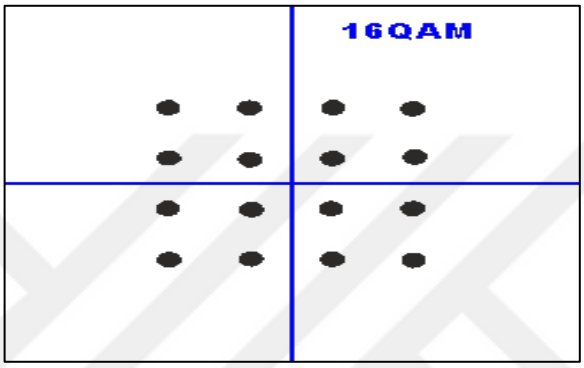

Figure: 2.5: 16QAM Constellation.

This QAM constellation diagram illustrates how the point spacing on the constellation decreases with increasing modulation order. Therefore, even a small quantity of noise might result in a larger issue; the larger the area a point on the constellation covers, the higher the noise level caused by the weaker signal. If it grows too big, the receiver will have trouble locating the broadcast signal in the constellation, which could result in mistakes. Additionally, it has been discovered that the amount of amplitude variation on the transmitted signal increases with the QAM signal's modulation order. Being a highly ordered modulation type, QAM has the benefit of enabling more data to be conveyed per token. The power spectrum efficiency and modulation bandwidth of higher-order QAM formats are comparable to those of M-formed PSK-ray formats, which means that for the same phase-shift switch configuration, square-amplitude modulation and phase-shift switch both have the same levels of power spectrum efficiency and bandwidth. Higher order modulation rates can lead to much quicker data rates and greater levels of spectrum efficiency for the radio communications system, but these advantages come at a price. The higher order modulation schemes are far more prone to noise and interference. This has led to the widespread use of dynamic adaptive modulation techniques in radio communications systems today. To get the highest data rate possible under the given

conditions, they identify the channel characteristics and adjust the modulation technique. As errors increase and more data must be delivered again as signal to noise ratios deteriorate, throughput will slow. By lowering data errors and resending's, switching back to a lower order modulation approach will increase the link's dependability. When a high level of resends are required due to data mistakes that occur when a high order modulation scheme is used, it is likely that the data rate will drop below that of the lower order modulation level. The best throughput for the current network conditions can be reached by choosing the appropriate order of QAM modulation and having the flexibility to dynamically change it. Lower bit error rates can be accomplished by reducing the order of the QAM modulation, which lowers the amount of error correction needed [76]. The throughput can then be maximized for the current link quality. Today, the majority of wireless communications systems, including Wi-Fi, mobile communications, and many other data transmission channels, accept and incorporate dynamic adaptation of the sequence of modulation as an essential component.

2.3 OFDM

Orthogonal Frequency Division Multiplexing disperses data information using a large number of low-rate sub-carriers. OFDM's resistance to channel dispersion and ease of estimating the phase and channel in a time-varying environment are some of its main advantages. Wireless LAN and digital audio/video broadcasting (DAB/DVB) are two RF applications that have benefited from the development of reliable silicon DSP (LAN) technology. However, OFDM has two inherent flaws: sensitivity to frequency and phase noise, and the maximum to average power ratio (PAPR) , the bit-rate digital information signal R_b is converted into $M = n^2$ symbols using (OFDM) (Each symbol represents a complex number that represents the M-array modulation scheme's amplitude and phase), divides the generated symbol stream (rate $R_s = R_b/n$) into N concurrent streams, each with a R OFDM rate equal to Rs/N, and modifies every stream onto a different N carrier , Each parallel information flow can be retrieved independently thanks to the N frequencies of the mutually orthogonal carriers during one OFDM symbol period, $TOFDM = 1/ROFDM$. In the figure below (Figure2.6) shows the spectrum of a few nearby(unmodulated) OFDM carriers.

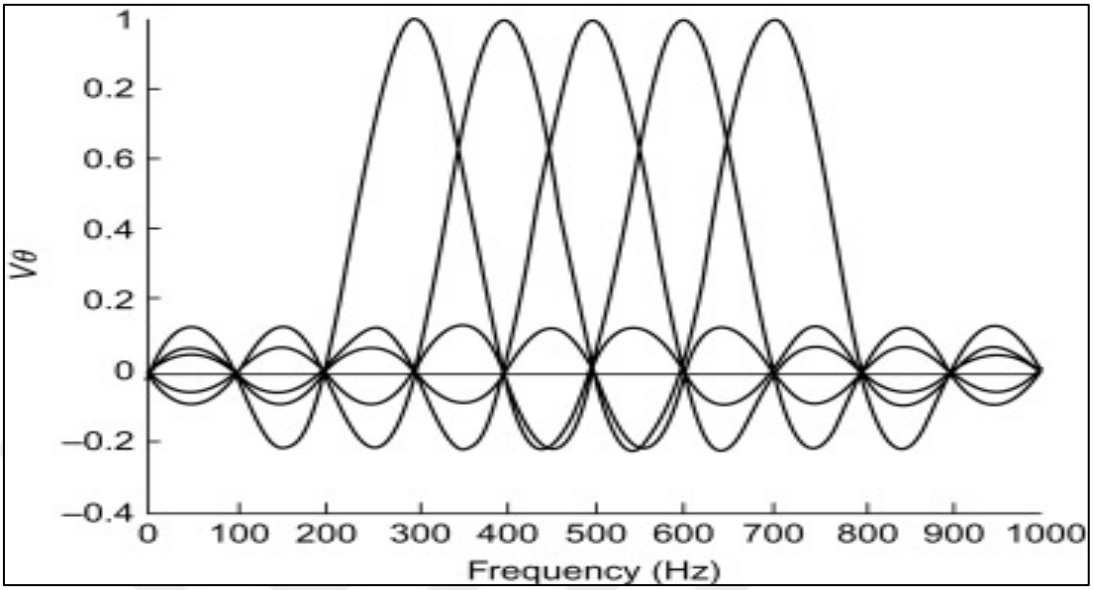

Figure 2.6: Five adjacent (unmodulated) OFDM carriers.

And to show the basic process of multiplying parallel symbol current on orthogonal carriers as shown in figure below (Figure 2.7).

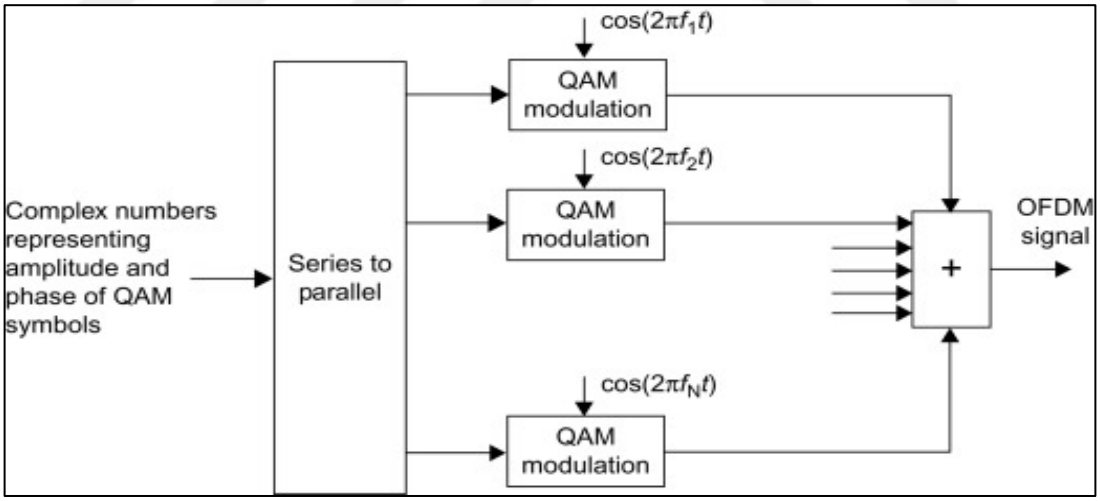

Figure 2.7: Conceptual representation of OFDM transmitter.

This is OFDM's main advantage since the original symbol stream's symbol rate is N times lower than the symbol rate of this one and Nn is less than the original bit stream. Early codes may overlap with later codes due to the radio channel's time dispersion, which is brought on by energy flowing between the transmitter and receiver over various paths, some of which include

reflection from far-off objects (ISI). By lowering each orthogonal channel's symbol rate (calculated as a percentage of the OFDM symbol time), the interference's negative effects on BER are significantly lessened. Real experiences show that phase noise and frequency offset cause the (SNR) for (OFDM) systems to degrade Each OFDM token can be made to last longer by adding a "periodic prefix" to maintain orthogonality. The prefix is a copy of the final segment that is added to the OFDM code. Prefix must be at least as long as the largest delayed (significant) multipath echo in order to be genuinely effective. One of the advancements that has made OFDM a more appealing alternative for radio communication in challenging multipath environments is the (extremely successful) Fast Fourier Transform (FFT) approach. The capacity and phase of a carrier are determined by the impact of the symbols combined number on that carrier. The amplitude and phase of the OFDM signal spectrum are thus determined by (N) of these symbols for one period of OFDM symbols (at different carrier frequencies). Thus, the FFT can be used to retrieve (demultiplex) symbols in the receiver and the fundamental OFDM signal in the sent can be produced using the inverse Fast Fourier transform. A rectangular pulse shape is used by Cyclic Prefix (OFDMCP-OFDM) for example, $p[n]$ is given by:

$$p[n] = \{_{0}^{\frac{1}{\sqrt{N_{SC}}}} \quad \text{if } 0 \leq n \leq N_{SC} - 1 \tag{2.1}$$

the total number of subcarriers is whereN_{SC}. There isn't a postfiltering process of

$$w_{TX}[N] = \delta[N]$$

The OFDM symbol is given a Cyclic Prefix (CP) in order to reduce Inter Symbol Interference (ISI) in a multipath channel, the received OFDM signal is free from ISI if the CP length is configured to be longer than the channel's delay spread. The process of connecting the final samples of an OFDM symbol, N_{cp}, to the symbol's front is referred to as "CP".

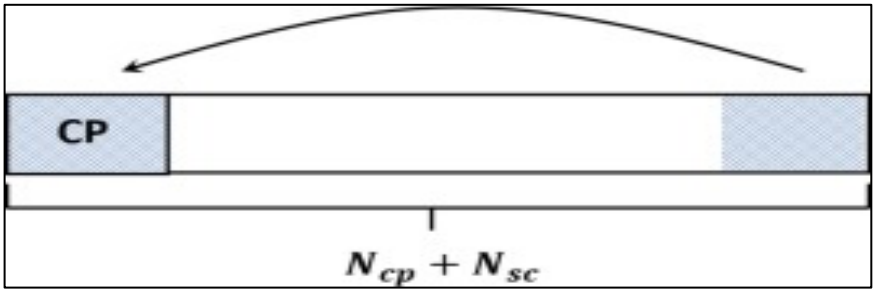

Figure 2.8: Add Periodic Prefix.

In practice, the (FFT) used to construct the CP-OFDM modulator (FFT). The transfer of M modulated QAM symbols ($\{X_i\}_{I=1}^{M}$) to orthogonal subcarriers is shown in (Figure 2.8) and consists of a (P/S) conversion, an IFFT of size N, and a (S/P) translation. Out of the total N subcarriers in this situation, M subcarriers are actively transferring data. To make filtering processes easier, the number of active subcarriers is often kept lower than the total number of subcarriers, as demonstrated in (Figure 2.9) [77]. this is accomplished by zero padding QAM symbols before the IFFT process.

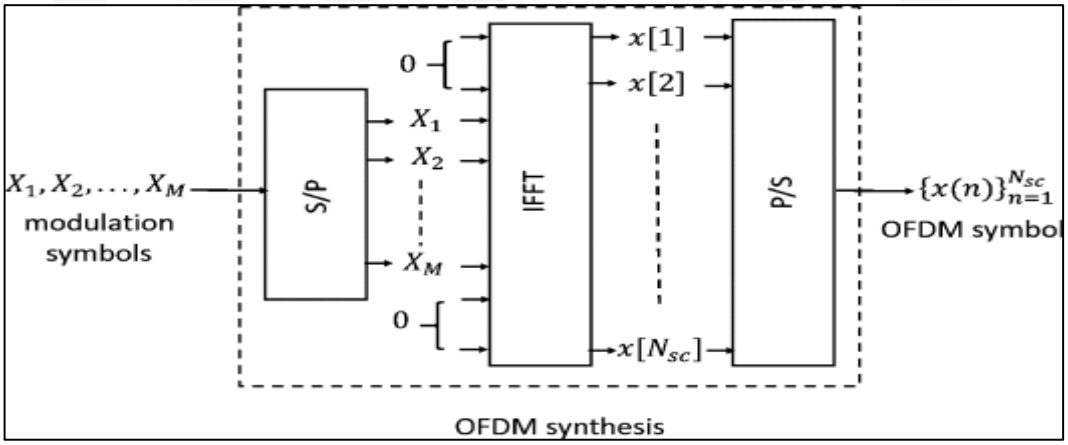

Figure2.9: Effectively use the Fast Fourier transform to create an OFDM waveform.

Using the modulation and multiplexing method of OFDM, it is possible to split up a single high data rate stream into multiple smaller data rate streams and send them across a single narrow sub channel. Both current applications and communication require high data speeds, transmission specifications, and system necessities. One of the most crucial and successful strategies is OFDM, Because OFDM divides the entire bandwidth into narrowband subcarriers

that are each smaller than the coherence bandwidth, the channel responses exhibit flat fading. Multiple low-speed broadcasts can be sent simultaneously while avoiding Inter-Symbol Interference (ISI). thanks to a network technology called OFDM. Thus, network throughput is increased (ISI). The subcarrier frequencies of OFDM are chosen to be orthogonal to, which greatly simplifies the transmitter and receiver designs. Due to the orthogonality, the spectral efficiency is good, and the total symbol rate is nearly equal to the Nyquist rate for the same baseband signal. The frequency range can be used almost entirely. Frequency synchronization and interference cancellation are the two methods used most frequently to reduce ICI in typical OFDM systems. The fact that they are typically very sophisticated makes them susceptible to bandwidth efficiency problems. By combining the (IFFT) at the transmitter and the (FFT) at the receiver to transform the wideband signal subject into N narrowband flat fading signals using frequency selective fading, the OFDM system reduces equalization complexity [78]. To do this, modest data rates are combined to produce high data rates with a lengthy symbol period.

2.4 CHANNEL MODEL

In order to satisfy the requirements of the fifth generation of communications, the Cluster Delay Line (CDL) channel concept is composed of numerous unique groups of delayed beams, each of which consists of a num. of multiple route components. the estimated delays, arrival angles, and angles are all the same despite the different departures. The change in beam angle could be due to the mobile's different base station. The terminal and displacement angles for each beam are represented by a Laplacian, in addition to the sending and receiving antenna's specifications, the CDL model considers all elements that have an impact on the signal traveling via the communication channel. (In this instance, massive MIMO technology), The received signal in the actual world typically includes a direct path in addition to the multi-path signal. routes, which vary in quantity and rely on how the electromagnetic wave interacts with nearby obstructions. These waves get there with various delays, and the signal obtained at the receiver (the receiving antenna) corresponds to the total of these waves. In specific situations, such those that occur indoors, it's feasible that the Line-of-Sight (LOS) isn't always present. Since the signal's amplitude and phase are changing, Non Line of Sight (NLOS) channels are used to facilitate communication in this scenario. The fundamental propagation phenomena witnessed

and the concept of multipath propagation are both shown in (Figure 2.10). The NLOS propagation scenarios are classified into 3 categories, namely CDL-A , CDL-B and CDL-C, We have shown that the three models differ in terms of usage scenario, [79] comprises all the content, including formulas and tables, for a frequency range between 0.5 and 100 GHz and channel bandwidth up to 2 GHz. The channel model is a crucial component of wireless communication system design and testing. IEEE 802.16m's channel model is anticipated to have a wide bandwidth, a high data rate, many antennas, and other elements because it aspires to satisfy IMT-Advanced criteria. Because different test settings have varied channel properties, test environments are an important consideration in channel modeling. Several test scenarios, including urban macro cell, suburban big cell, urban micro cell, indoor small office, and outdoor to indoor environments, have been designed to replicate and evaluate IEEE 802.16m systems, another significant possibility hasn't yet been found or predicted, though. The mobile cellular system will become "hotspot" cells, or cells with a high traffic density, when the traffic load develops unevenly more than the intended load. Hotspot test environments focus on deployment conditions in urban centers with highly rated tall buildings and wider pedestrian streets, as well as taking into account rating factors such as a large number of users. Antenna geometry and propagation parameters can be separated using geometry-based radio channel modeling. Spatial Extension of Delay Line (TDL) Models Details of the power, delay, and Doppler spectrum of taps are usually included in TDL models. Power, delay, and angle information is determined by CDL models. Since it is determined by energy and angle information along with matrix configurations, Doppler is not formally defined. Each group in the CDL model consists of 20 beams of identical energy with predetermined offset angles. When there is a dominant ray in a block, then the block has 20 + 1 ray. This dominant ray has a displacement of zero degrees. A random coupling occurs between the arrival and departure rays., are the relevant CDL tables. CDL models offer clearly defined radio channels with preset characteristics in order to get simulation results that are comparable with relatively simple channel models for calibration purposes. The CDL parameters for LOS and NLOS circumstances are listed in table (2.1). In the LOS model, the first and second clusters' respective Ricean K factors are 15.3 dB and 10.4 dB [80].

Table 2.1: LOS Clustered Delay Line Model, Indoor Hotspot.

cluster	delay[NS]	power [dB]	AoD [°]	AoA [°]	Ray Power [dB]		Cluster ASD = 5°	Cluster ASA = 8°
1	0	0	0	0	-0.1*	- 28.4**		
2	5	- 3.4	64	- 73	- 3.7 *	- 27.1**		
3	10	-9.2	115	80	- 22.2			
4	20	-18.9	7	13	-31.9			
5	30	-17.1	11	16	-30.1			
6	40	-16.3	-7	-34	-29.3			
7	50	-13.7	-60	-12	-26.7			
8	60	-16.3	-43	-17	-29.3			
9	70	-16.8	11	-59	-29.8			
10	80	-17.9	8	-78	-30.9			
11	90	-15.9	14	-65	-28.9			
12	100	-17.4	-1	-56	-30.4			
13	110	-25.8	-11	-57	-38.8			
14	120	-31.0	-129	-22	- 44.0			
15	130	-33.4	-123	-12	- 46.4			

2.5 CHANNEL ESTIMATION

The LMMSE, which has good estimation performance for all SNR values, is used in this study to estimate the channel. It is frequently used in the theoretical analysis and practical

implementation of MIMO systems [81]. Additionally, It offers an estimation error that is straightforward to comprehend and useful for examining system performance limits because it is statistically orthogonal to the estimation. However, for the LMMSE channel estimator to perform at its best, a thorough understanding of the channel correlation matrix is necessary. This information is typically considered to be available in the receiver in the literature, despite the fact that the effort needed in calculating the channel and the channel correlation matrix are separate activities. The correct estimate of correlation matrices is very crucial for many applications. This statistical problem is based on a sample of data and involves a stochastic process. However, in order to achieve a reliable computation of the channel correlation matrix, we must monitor a large sample set over a long period of time, encapsulate the channel's second order invariant characteristics. In many instances, the channels' time actually slowly changes. In addition, the time allocated for transmitting training data is sometimes only partially constant, to be compact in order to preserve the system's overall efficacy. Additionally, the channel is not fixed in some diffusion circumstances, such as vehicle transportation, and then Over time, the channel correlation matrix could alter [82].as a result, it is likely that the LMMSE channel estimator will be utilized in practice with an erroneous estimate of the channel correlation matrix. The indicative distribution was chosen to trace the temporal and frequency fluctuations of the channel more accurately. A block-type empirical arrangement (for quasi-static channels), a comb-type pilot configuration, or a hexagonal empirical arrangement are all frequently considered in the literature (for frequency- and time-selective channels). LMMSE channel estimation can be done independently along the frequency and time axes for both mass and comb-type layouts. With a pilot preamble, the LMMSE estimation is carried out along the frequency axis. a matrix, and therefore requires the optimization of its coefficients, is produced by minimizing the cost function. The channel's anticipated frequency response is written.

$$\text{as} J_{\text{MMSE}} = E\{\| \boldsymbol{H}_n - \underline{\boldsymbol{D}}\boldsymbol{Y}_n \|^2\} \tag{2.4}$$

Where $\underline{\boldsymbol{D}}_{\text{opt}} = \underline{\boldsymbol{R}}_{H_f}\underline{\boldsymbol{X}}_n^{\text{H}}(\underline{\boldsymbol{X}}_n\underline{\boldsymbol{R}}_{H_f}\underline{\boldsymbol{X}}_n^{\text{H}} + \sigma^2\underline{\boldsymbol{I}})^{-1}$ and $\underline{\boldsymbol{R}}_{Hf}$ is the covariance matrix for the $\underline{\boldsymbol{X}}_n$ frequency axis along the channel. is the matrix of the MxM identity and $(.)^H$.

the Hermitian transpose If the pilot vector according to [83]. the typical formulation of the LMMSE estimation is provided by (2.5) and is invertible.

$$\hat{\boldsymbol{H}}_n^{\mathrm{LMMSE}} = \boldsymbol{R}_{H_f}\left(\boldsymbol{R}_{H_f} + (\boldsymbol{X}_n\boldsymbol{X}_n^{\mathrm{H}})^{-1}\sigma^2\boldsymbol{I}\right)^{-1}\hat{\boldsymbol{H}}_n^{\mathrm{LS}}, \tag{2.5}$$

With H_n^{LS} is the vector that LS calculated to include the samples of the channel frequency response. Frequently, the noise variance is defined as $\sigma^2 = E\{|W_{m,n}|^2\}$ is anticipated to be known or precise calculated. The average pilots power is a highly common complexity reduction method for LMMSE that was first presented by Edfors et al. $E\{(\boldsymbol{X}_n\boldsymbol{X}_n^{\mathrm{H}})^{-1}\}$ instead of $(\boldsymbol{X}_n\boldsymbol{X}_n^{\mathrm{H}})^{-1}$, This is employed in the majority of articles addressing LMMSE estimation. that the prior approximation has very little impact on the LMMSE estimator's performance.

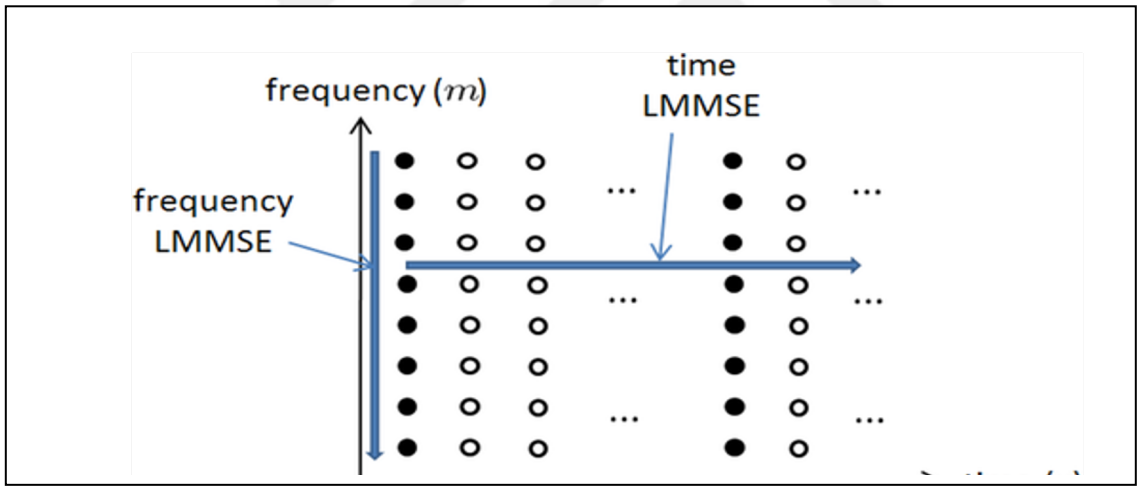

Figure 2.10: An example of the (2x1) dimensions LMMSE filter.

2.6 NEURAL RECEIVER

Recent developments in deep learning methods have given rise to fresh uses of neural networks in a number of industries, including wireless communications [83]. It is undeniable that the processing employed at the physical domain layer forms the cornerstone of overall performance at the network level. Therefore, there are a lot of unrealized gains in physical layer processing that can be made through the usage of DL, and we can take advantage of these advantages to improve the radio performance of specific network devices. Particularly, some specialized

reception challenges, such channel and equalization estimates, can both be taken into consideration by approaching the construction of radio receivers as a supervised learning issue. Instead of individually optimizing each component, it will be more efficient to train a deep neural network to recognize the received bits of the received waveform. Its objective is to extract data bits from a waveform that has been altered to meet 5G orthogonal frequency division multiplexing (OFDM) requirements, with this method, the receiver's work can be classified as a supervised learning problem without the aid of either existing algorithms or human classification. Shental and Hyoids developed a deep neural network method to compute effective bit-Log-Likelihood Ratios (LLRs) for equal symbols, which are effectively the basis for the initial bits that are supplied, as described in Effie [84]. It demonstrates how, although using much less processing power, a deep learning-based mapping technique may attain accuracy levels comparable to maximum log optimization for suffix. As long as the proper training is put in place, improving the traditional receiver's processing flow with deep learning components is preferable to the baseline performance of the traditional receiver. There, a fully linked neural network analyzes both the data stream and the pilots to carry out the detection. It is shown that a fully learned receiver outperforms a typical receiver in terms of Minimal Mean Square Error (MMSE) when there aren't many pilots to estimate channels or when the periodic prefix isn't there. which, at low to medium optical signal speeds, performs superbly. At high SNRs, the linear least squares-based receiver continues to perform better than the CNN-based system. But with the pixel-assisted MMSE-based receiver, the optimal channel knowledge does not happen as quickly. The most extreme example of prior attempts has been successfully built for comprehensive deep learning systems, where both the transmitter's and the receiver's wave structure or modulation scheme are simultaneously learned from the input. Furthermore, it performed better than more advanced futuristic algorithms. These findings demonstrate that a deep neural network-driven data-driven receiver can be built to enhance the functionality of future radio systems. However, it appears to be able to dramatically enhance performance by carefully modifying the neural network architecture and its inputs. In light of the findings, the neural network's ability to employ and distribute unknown data symbols in channel optimization Estimation accuracy is what produces the majority of the improvements. Unlike many other efforts, this one additionally considers compliance with standards, especially with

5G New Radio (NR). Acquired receivers must, among other things, Support Modulation Extraction References (SMRS) or experimental configurations described in the NR specification in order to be 5G compatible. A low-density symmetry-checking (LDPC) decoder must also decode the receiver's output. This calls for the neural network to have the ability to calculate the uncertainty for each received bit for each modulation order. Future solutions based on deep learning that are adaptable and can manage a variety of bookmark configurations and modification plans in a single implementation while adhering to other processing steps are thus required. Here, we shift our attention to the Rx-NN network architecture's architectural principles. The final bit-level LLRs are produced by Rx-NN using the Fourier converted frequency-domain data acquired during a e Transmission Time Interval (TTI). The network can use all the data in the TTI to estimate each bit if the entire TTI is inputted at once. Due to the non-static environment and perhaps mobile UEs, each subcarrier and OFDM symbol's frequency-domain channel coefficients are also distinct. Given that the physical channels in these circumstances exhibit significant local correlations in both frequency and time, a fully convolutional neural network is one in which 2D convolutions function in both these dimensions. These 2D CNN filters are designed to pick up on these local correlations, which are independent of frequency and time, and to make efficient use of them throughout the TTI. Another reason for the architecture is that since the sparse pilot symbols only provide local channel information, by allowing the network use the unknown data and its known distribution, we may be able to use it to more accurately forecast LLRs far from the real pilot positions. Consequently, in contrast to other previous methods, instead of creating separate conduits or blocks for pilot-based channel estimation and data symbol equalization, we provide CNN unfettered access to all data. Because this enables the network to use all of the data to fulfill the assigned task, we hypothesize that the channel and LLR estimation can be improved if the entire TTI (both the unknown received data and the known pilots) is delivered to the network in a coherent manner. The following explanation applies to a MIMO scenario, however, it is also possible to use this design concept in a MIMO operation where multiple signal streams are spatially multiplexed. Our first aim is to fully utilize the Rx-NN architecture's MIMO processing capabilities. Incoming data and pilot information are combined to create a three-dimensional input array as seen in figure below (Figure 2.11), and the basis for Rx-functioning

is this knowledge. The received signal following the FFT is the first component of the input for NN's, denoted by $Y \in C^{S\,x\,F\,x\,N^r}$ S, which includes both data and pilot symbols received, is the quantity of symbols in time, followed by F, the num. of subcarriers, and Nr, the num. of RX antennas.And The second part is $X^P \in C^{SxF}$ The non-pilot points in the received signal Y are matched by the pilot reference symbols in both frequency and time, with the non-pilot locations filled with zeros.

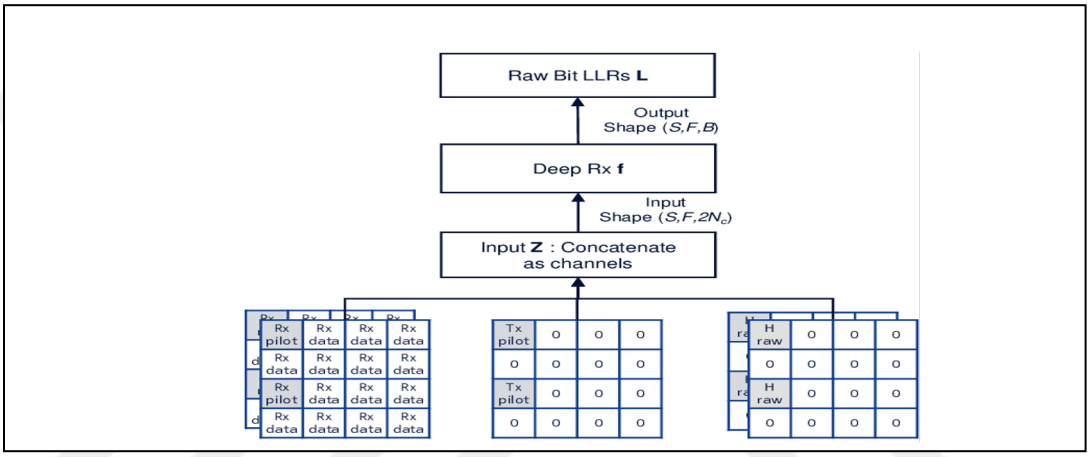

Figure 2.11: The raw channel estimations, the known pilot symbols, and the received unknown data are concatenated as the input to the Rx-NN.

Additionally, we compute the raw the third dimension, the components of Xp are repeated. channel estimates beforehand. $\widehat{H}_r = Y \odot X_P^*$ for the positions of pilots, where $\odot$ and $(.)^*$ offer this as the third input. are, respectively, the complex conjugate and the element wise product. If there are many, when conducting the raw channel estimates RX antennas, the third dimension, the components of Xp are repeated. Since the initial two dimensions of Y, Xp and $\widehat{\widehat{H}_r}$ if they are equivalent, they can be stacked with the third dimension (channel) to create $Z \in C^{S\,x\,F\,x\,N_C}$ where $N_C = 2N_r + 1$ Furthermore, The final input array is created by stacking the real and imaginary portions of the input as separate channels and converting the complex-valued input to real-valued $Z \in R^{Z\,x\,F\,x\,N_c}$ The convolutions can function on related data by stacking the pertinent information into channels in this way. Although another alternative is to use a complex-valued network with a complex-valued input, we haven't seen any performance benefits from doing so. To a normalized CNN array with residual connections for the neural

network $f: Z\ L$, where L is the matrix holding the outputs of LLRs, we apply a ResNet pre-reactivation neural network. Time and frequency are the first two dimensions that are used in 2D convolutions. Because the structure is entirely convolutional, the output size ($S\ F$), Even for each TTI when employing the same trained neural network, the input size can change immediately. It is necessary in particular to compute the LLR estimations for each symbol in the input. The network does not use maximum pooling or scaling, which are typically used in CNNs to degrade resolution, as a result, maintaining constant resolution (S F). Remember that the input size can be raised from the training set but shouldn't be decreased from the full field because convolutions with zero padding may have unexpected effects on the output. As opposed to changing the resolution, we add more filters to the network's intermediate layer and use extended convolutions to boost for instance, semantic segmentation frequently involves the receptive domain [85]. Stretching, as opposed to scrolling, enables the network to collect longer relationships in time and repetition while preserving complete information about each input token. Expansions turned out to be especially crucial for shallow buildings. Additionally, we noticed better outcomes when deeply detachable gyres [86]. were used in place of conventional gyri. The depth 2 multiplier for profoundly detachable gyri is used to obtain the major results in this study, which effectively means that the depth convolution's output channel count is doubled to increase the amount of parameters and improve the network's modeling capabilities. Finally, a straightforward binary classification problem is used to describe the prediction of bits. The bit LLRs $L \in R^{SxFxB}$, where B is the quantity of bits in the constellation being utilized , make up the Rx-NN's final result (e.g., 4 for 16 QAM). For the purpose of calculating the loss between each ground truth bit and the network output L, we use the binary sigmoid Cross-Entropy (CE) method.

$$CB(\emptyset) \triangleq -\frac{1}{\#DB}\sum_{(i,j)\in D}\sum_{l=0}^{B-1}(b_{i,jl}\log(\hat{b}_{ijl}) + (1-b_{i,jl})\log(1-\hat{b}_{ijl}) \qquad (2.6)$$

where $\#D$ is the quantity of data-carrying resource elements. and $b_{i,jl}$ is a prediction of the likelihood that the bit $b_{i,jl}$ is one,

$$b_{i,jl} = sigmoid\ (L_{ihl}) = \frac{1}{1+e^{-L_{ihl}}} \qquad (2.7)$$

The architecture of Rx-NN CNN ResNet as mentioned in (Table 2.2).

Table 2.2: The Rx-NN CNN ResNet Architecture.

Layers	**Types**	**Filter (S, F)**	**dilation (S, F)**	**Out-put shape**
In-put 1 $Y \in C$	$RX\ Data$	none	none	(S, F, Nr)
$Input\ 2\ Xp \in C$	$TX\ Pilot$	none	none	$(S, F, 1)$
$Input\ 3\ Hr \in$	Raw channel estimate	none	none	$C\ (S, F, Nr)$
$Input\ Zc \in C$	Concatenate inputs 1-3 ∈ C	none	none	(S, F, Nc)
$Real\ input\ Z \in R$	Concatenate ∈ R	none	none	$(S, F, 2Nc)$
Conv In	2D convolution	(3,3)	(1,1)	$(S, F, 64)$
ResNet Block 1	Depth wise Separable Conv.	(3,3)	(1,1)	$(S, F, 64)$
ResNet Block 2	Depth wise Separable Conv.	(3,3)	(1,1)	$(S, F, 64)$
ResNet Block 3	Depth wise Separable Conv.	(3,3)	(1,1)	$(S, F, 128\ )$
ResNet Block 4	Depth wise Separable Conv.	(3,3)	(1,1)	$(S, F, 128\ )$
ResNet Block 5	Depth wise Separable Conv.	(3,3)	(1,1)	(S, F, 256)
ResNet Block 6	Depth wise Separable Conv.	(3,3)	(1,1)	$(S, F, 256)$
ResNet Block 7	Depth wise Separable Conv.	(3,3)	(1,1)	$(S, F, 256)$
ResNet Block 8	Depth wise Separable Conv.	(3,3)	(1,1)	$(S, F, 128)$
ResNet Block 9	Depth wise Separable Conv.	(3,3)	(1,1)	$(S, F, 128)$
ResNet Block 10	Depth wise Separable Conv.	(3,3)	(1,1)	$(S, F, 64)$

Table 2.2: The Rx-NN CNN ResNet Architecture. "Tables continued"

Layers	**Types**	**Filter (S, F)**	**dilation (S, F)**	**Out-put shape**
ResNet Block 11	Depth wise Separable Conv.	(3,3)	(1,1)	$(S, F, 64)$
Conv Out-put	2D Convolution	none	none	(S, F, B)
LLR Output L	Out-put	none	none	(S, F, B)

3. RESULTS & DISCUSSION

3.1 SIMULATION SETUP AND PARAMETERS

We simulate the proposed system in order to train the Neural receiver that detect OFDM, where channel estimation and valence and neural receiver mapping are replaced. creates the received resource network by computing (LLRs) on the sent encoded bits using samples obtained after discrete Fourier transformation (DFT). The LLRs are then provided to an external decoder to reproduce the transmitted data bits used in the simulations. Then we set up an accurate simulation of a mobile User Terminal (UT) and a point-to-point (BS) MIMO link of the base station. Up and down trends are taken into consideration. One of the Python programming language libraries Sionna, an open-source library built on Tensor Flow for physical layer modeling of wireless and optical communication networks, is used to carry out the simulation. Connecting the appropriate building blocks, which are offered as Keras layers, allows for rapid prototyping of complicated communication system structures. Gradients can be distributed throughout an entire system by employing differentiable layers, which is a crucial tool for machine learning, particularly neural network integration, and system optimization. It allows for the simulation of MU-MIMO, links using (LDPC), Polar en/decoders, 3GPP channel models, and OFDM codecs that are compatible with 5G. (OFDM). It also provides channel estimates, equalization, and soft map removal. The system parameters used in the simulations are shown in Table 3.1.

Table 3.1: System Specific Simulation Parameters.

Description	Value	Description	Value
Number of UT	1	Carrier frequency	2.6e9
Num. of BS	1	Delay spread	300e-9
Num. of UT antenna	4	Cdl model	A-B-C-D-E
Num. of BS antenna	8	Speed	10
Num. of OFDM symbols	14	FFT size	128
Subcarrier spacing	$15e^3$	Number bits per symbol	2
Cyclic prefix length	6	Number convolutional channels	128

3.2 STREAM MANAGEMENT

Any type of MIMO simulation can benefit from setting a stream management object. We will build up one UT and one BS with a choice of antennas in each based on the transmitters and receivers that exchange data streams with one another. Depending on the direction, which could be uplink or downstream, UT or BS are considered as either transmitters or receivers. Precoding and Equalization are just two of the many features that Stream Management has and that other parts use. Here, we will set up the system so that the num. of transmitter streams (uplink and downlink) equals the num. of UT antennas.

3.3 OFDM RESOURCE GRID & PILOT PATTERN

A grid of OFDM resources that spans many OFDM symbols is created. Data symbols and pilots make up the resource grid, which in 4G/5G parlance is comparable to a slot. Even though they are not crucial to our situation, A few guard carriers are also present to the left and right of the spectrum, we null the DC subcarrier. A cyclic prefix is also utilized. a Pilot Pattern is created automatically when the Resource Grid is created. An approach would have been to first create a Pilot Pattern and then supply it as a startup parameter, and this result of OFDM resource grid as shown as in figure below (Figure 3.1).

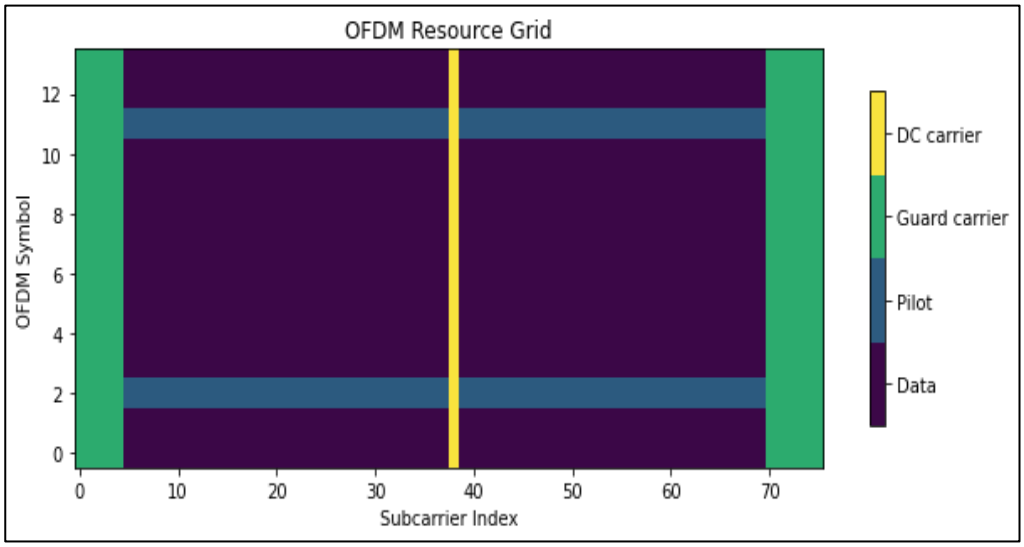

Figure 3.1: OFDM resource grid.

The resource grid, which can be seen in the image above, has 76 subcarriers spread across 14 OFDM symbols. To the left and right of the spectrum, every guard carrier, including a DC guard carrier, are nulled. Pilot transmissions employ the third and twelfth OFDM signals. Let's take a look at the transmitter's pilot pattern, and this result of pilot pattern as shown as in figure below (Figure 3.2).

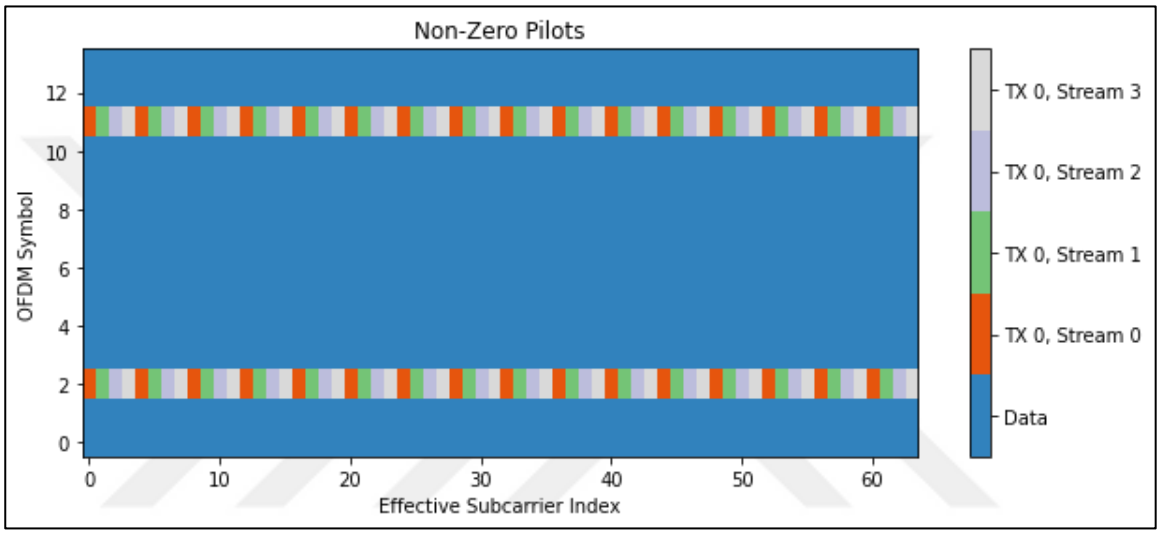

Figure 3.2 Pilot Pattern.

Pilot programs are made available to DC carriers and functional subcarriers from whom the shield has been removed across the whole resource network. This yields 64 functional subcarriers in our example, 66-2 (left guard) and 76-1 (DC) (right guard). The resource network only knows which resource items are reserved for pilots; the pilot pattern determines what is actually transmitted to them. In our case, the Kronnecker Pilot Pattern and four dispatch streams are configured. There is a pilot on every fourth subcarrier in orthogonal pilot sequences, which are normalized so that the average power of each pilot symbol is equal to one. The amplitude is adjusted by a factor of two because the sequence only uses a beta sign for per fourth iteration, and this result of pilot sequences as shown as in figure below (Figure 3.3).

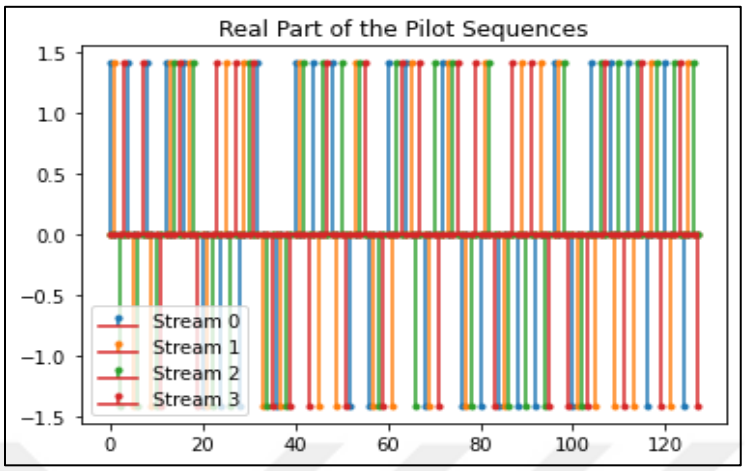

Figure 3.3: Pilots Sequences.

3.4 ANTENNA ARRAYS

In the process of configuring antenna arrays used by developers UT and BS. The geometry of antenna arrays and antenna radiation patterns are taken into account. For the 3GPP 38.901 specification's CDL, UMi, UMa, and RMa models, this is necessary. In this section, we'll assume that the UT and BS antenna arrays are made up of dipole antenna components that adhere to the 3GPP 38.901 antenna configuration. By default, the vertical and horizontal spacing between antenna elements is half a wavelength. If necessary, you can create your own antenna configurations and radiation patterns. The y-z level is where the Antenna Array is always specified. The direction of UT or BS will decide its final direction, and this result of the antenna array to BS and UT as shown as in figure below (Figure 3.4).

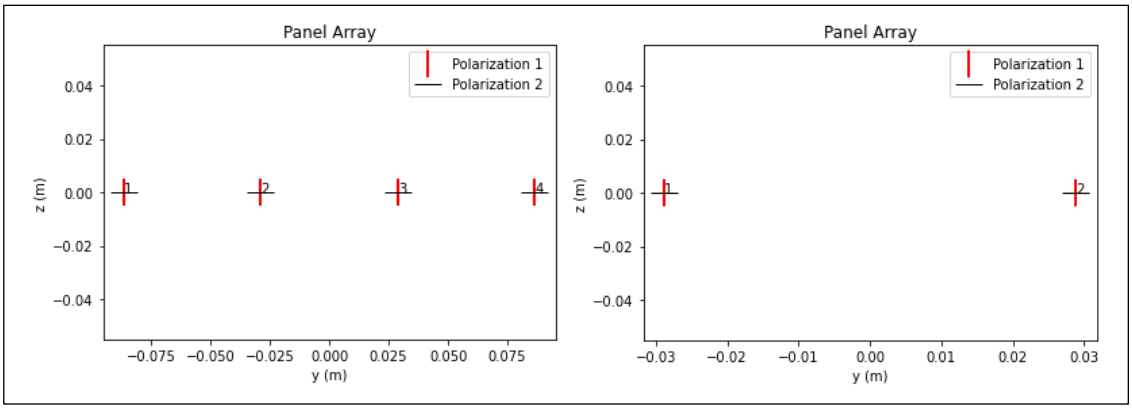

Figure 3.4: the Antenna Array to BS& UT.

3.5 CDL CHANNEL MODEL

As soon as the CDL Channel Model is generated, an example of the CDL Channel Model with complicated gains a and tau delays for each path, continuous time channel pulse replies can be produced using CDL in batches that are randomly realized. The channel pulse responses are gathered at the sampling frequency for the required amount of time samples in order to produce time-varying channels. Channel simulation in the frequency domain, we need a number of symbol samples from DM symbols taken once for each OFDM symbol duration, which is equal to the OFDM symbol length plus the periodic prefix. It is projected that during the time-window of interest, the delays won't alter, only the advantages of challenging paths change over time. The next two figures, respectively, depict the channel impulse response at a certain time instant and the gain of one path as it varies over time, and this result of the channel impulse response as shown as in figure below (Figure 3.5).

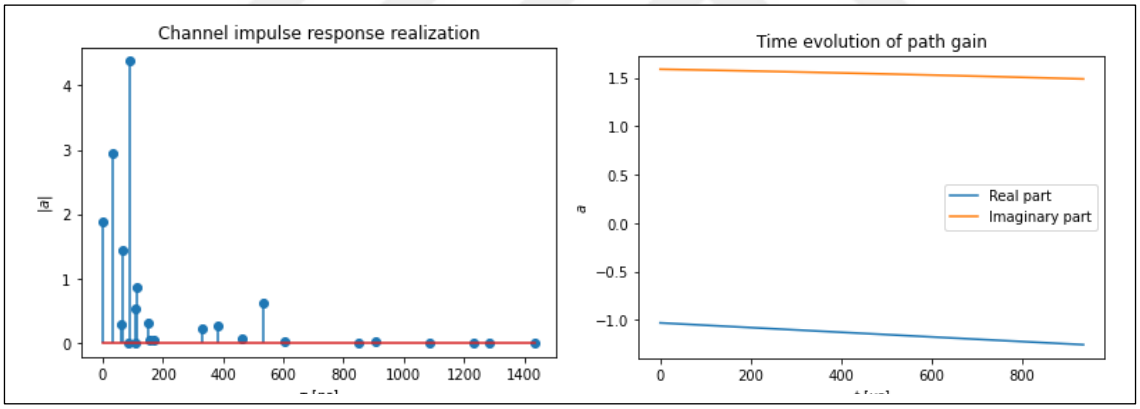

Figure 3.5: the channel impulse response.

3.6 RX-NN RECEIVER

It creates the Keras layer, which controls the neural receptor. the neural receives the 2D resource network as an input and must effectively handle it, the remaining convolutional layers are elevated, before the next stage of defining the Keras layers that implement the neural receives takes place. Avoiding gradient fading is accomplished using residual joins (skipping). For ease of use, a residual block's implementing Keras layer is initially defined. This Keras layer produces a convolutional residual block by stacking these blocks, there are two convolutional layers paired with (ReLU) activation, layer normalization, and a skip connection. In order for

the skip connection to work, the constant "NUM. CONV CHANNEL" implies that the input's convolutional channels' number and the convolutional layers' number must be equal. The residual convolutional neural receiver is added to the Keras layer. using the post-DFT received samples as input, Using the transmitted coded bits as input, this neural receiver computes LLRs to create a resource grid of dimension numb. of symbols $x\ fft$ size. The information bits can then be reconstructed using these LLRs as input to a decoder. The guard bands and pilots are included in the resource grid given to the neural receiver, which also computes LLRs for these resource elements. To just keep the essentials, they must be discarded.

3.7 END TO END SYSTEM AS A KERAS MODEL

The three systems under consideration—the perfect CSI baseline, the LS estimation baseline, and the neural receiver—share the majority of the associated components, hence an end-to-end Keras model is adopted (transmitter, channel model, external code, etc.). The system to be setup is specified by the 'System' parameter of a Keras model, and the 'Train' parameter determines whether the system has been instantiated for training or assessment. Only when the channel realizations are randomly chosen, applied to the channel input, and the neural component in each call of this model is a set of randomly chosen code-words that are shaped and assigned to resource networks to construct the channel input, is the "training" parameter meaningful, and the receiver is used to compute the LLRs on the encoded bits on the post-DFT samples that were received. If training is not done, an external decoder is utilized to reassemble the information bits. The specified "system" parameter defines which receiver is used (baseline with complete knowledge of CSI, baseline estimate LS, or neural receiver). To estimate the batch BMD, transmitted bits and LLRs are employed, if trained.

3.8 EVALUATION OF THE BASELINES

The proposed Rx-NN-based receiver is compared with two conventional LMMSE receivers, the first of which is referred to as a practical LMMSE receiver since it completes channel estimation using data codes and subcarriers, and the BER rates reached by baselines are examined, and the second that receives channel information Complete as prior knowledge. The first estimates the upper limit of performance that can be achieved using the LMMSE equation.

For both conventional receivers, including one with perfect channel knowledge, we use the approximate rule and the main reasons for this is the fact that the LMMSE receiver with perfect channel information uses OFDM receiver process processing, which means that it sometimes cannot achieve perfect balance and interference caused by Doppler between carriers and changes in the primary channel within each element of the resource, the primary performance criterion for this model is Bit Error Rates (BER). Specifically, we take into account the encoded BER produced by running the LLRs through a modified decoder before a 5G compliant LDPC decoder and contrast the encoded bits with the original bit sequences. If the LLRs offered by the Rx-NN for LDPC decoding appropriately capture the uncertainty in the observed bits, they can be identified by the encoded BER analysis. The validity of the LLRs themselves can also be inferred from the encoded BER, since there is no ground truth, direct examination of LLRs is challenging (Under the used channel models, an explicit formula for ideal LLRs does not exist). Using the correlation simulation data, the model was trained. The main learning rate is first adjusted to the random initialization 102, and we also apply a little weight decay with a scale factor of 104 to avoid increasing the amounts of weight over a long training period. The optimization is performed using the LAMB optimizer [87]. When using four 2080Ti GPUs in parallel, LAMB allows the training size to be scaled up to larger batch sizes (eg 80 TTIs, 312 x 14 x 8 bits each, or 28 million bits per batch resolution), but not to smaller batch sizes (eg),) while Adam [88] may also run in batches of 20 TTIs or less. The linear learning rate warm-up time from zero to the main learning rate, which lasts 800 iterations, should also be used for large batch sizes. In addition, after 30% of the total iterations, the learning rate drops linearly to zero. In general, we typically run 10,000 iterations with a batch size of 80 TTI, and longer runs did not yield significantly better results.

When evaluating the (BER) rates achieved by the system baselines, we note in (Table 3.2) that the received (BER) as equal = 0 at Eb/No = 4.5 when using LS channel estimation with neare st-neighbor LMMSE equalization as a baseline at the receiving end in the process.

Table 3.2: Simulation Output Baseline LS Channel Estimation

Eb/No [dB]	BER	BLER	Bit errors	Num. bits	Block errors	Num. blocks	Run time[s]
-5.0	2.5356e-01	1.0000e+00	45178	178176	128	128	5.6
-4.5	2.3475e-01	1.0000e+00	41826	178176	128	128	0.4
-4.0	2.1828e-01	1.0000e+00	38893	178176	128	128	0.4
-3.5	1.9420e-01	1.0000e+00	34601	178176	128	128	0.4
-3.0	1.6453e-01	1.0000e+00	29315	178176	128	128	0.4
-2.5	1.0301e-01	9.8438e-01	18354	178176	126	128	0.4
-2.0	2.1271e-02	5.3516e-01	7580	356352	137	256	0.8
-1.5	9.2792e-04	2.9225e-02	4464	4810752	101	3456	9.6
-1.0	1.2527e-04	2.1875e-03	2232	17817600	28	12800	34.9
-0.5	4.4675e-05	3.9063e-04	796	17817600	5	12800	36.4
0.0	4.3833e-05	4.6875e-04	781	17817600	6	12800	35.1
0.5	1.0495e-05	7.8125e-05	187	17817600	1	12800	34.9
1	0.0000e+00	0.0000e+00	0	17817600	0	12800	34.6

The evaluation of the system, but in (Table 3.3), the error rate in the received bits equal = 0, t hat is, there is no error rate in the received bits at the value Eb/No = 1 when using perfect CSI as a baseline in the evaluation process of the system, but when using the neural receiver as a b ase line in the process of evaluating the system.

Table 3.3: Simulation Output Baseline Perfect CSI.

Eb/No [dB]	BER	BLER	Bit errors	Num. bits	Block errors	Num. blocks	Run time[s]
-5.0	3.8958e-01	1.0000e+00	69414	178176	128	128	5.5
-4.5	3.8202e-01	1.0000e+00	68066	178176	128	128	0.4
-4.0	3.6833e-01	1.0000e+00	68066	178176	128	128	0.4
-3.5	3.5541e-01	1.0000e+00	63326	178176	128	128	0.4
-3.0	3.4102e-01	1.0000e+00	60761	178176	128	128	0.4
-2.5	3.2717e-01	1.0000e+00	58293	178176	128	128	0.4
-2.0	3.1188e-01	1.0000e+00	55569	178176	128	256	0.4
-1.5	2.9299e-01	1.0000e+00	52204	178176	128	3456	0.4
-1.0	2.7783e-01	1.0000e+00	49503	178176	128	12800	0.4
-0.5	2.5763e-01	1.0000e+00	45904	178176	128	12800	0.4
0.0	2.3102e-01	1.0000e+00	41162	178176	128	12800	0.4
0.5	1.0495e-05	1.0000e+00	36168	178176	128	12800	3.0
1	0.0000e+00	1.0000e+00	30140	178176	128	12800	0.4
1.5	9.0624e-02	9.3750e-01	16147	178176	120	12800	3.0
2.0	1.2953e-02	2.4609e-01	9232	712704	126	512	1.4
2.5	8.2717e-04	1.2401e-02	9285	11225088	100	8064	23.1
3.0	2.5132e-04	2.1094e-03	4478	17817600	27	12800	34.7
3.5	1.1983e-04	9.3750e-04	2135	17817600	12	12800	34.2
4.0	1.0563e-04	6.2500e-04	1882	17817600	8	12800	34.4
4.5	0.0000e+00	0.0000e+00	0	17817600	0	12800	34.2

We note, as in (Table 3.4), that the error rate in the received bits equal = 0 at Eb/No = 1, which is identical to the values when using perfect CSI as a baseline in the evaluation process of the s ystem and when compared with using LS channel estimation with nearest -neighbor LMMSE equalization as a baseline at the receiving end.

Table 3.4: Simulation Output Baseline Neural Receiver.

Eb/No [dB]	BER	BLER	Bit errors	Num. bits	Block errors	Num. blocks	Run time[s]
-5.0	2.6772e-01	1.0000e+00	47702	178176	128	128	0.3
-4.5	2.5147e-01	1.0000e+00	44806	178176	128	128	0.3
-4.0	2.3377e-01	1.0000e+00	41653	178176	128	128	0.3
-3.5	2.1260e-01	1.0000e+00	37881	178176	128	128	0.3
-3.0	1.8983e-01	1.0000e+00	33824	178176	128	128	0.3
-2.5	1.5238e-01	1.0000e+00	27151	178176	128	128	0.3
-2.0	1.8023e-02	5.3516e-01	14338	178176	122	128	0.3
-1.5	1.8023e-02	3.2292e-01	9634	534528	124	384	1.0
-1.0	2.7484e-03	4.5312e-02	4897	1781760	58	12800	3.2
-0.5	9.7432e-04	9.3750e-03	1736	1781760	12	12800	3.2
0.0	4.2654e-04	5.4687e-03	760	1781760	7	12800	3.2
0.5	2.5424e-04	2.3437e-03	453	1781760	3	12800	3.7
1	0.0000e+00	0.0000e+00	0	1781760	0	12800	3.2

We notice that the neural network device is significantly superior, according to the figure below (Figure 3.6).

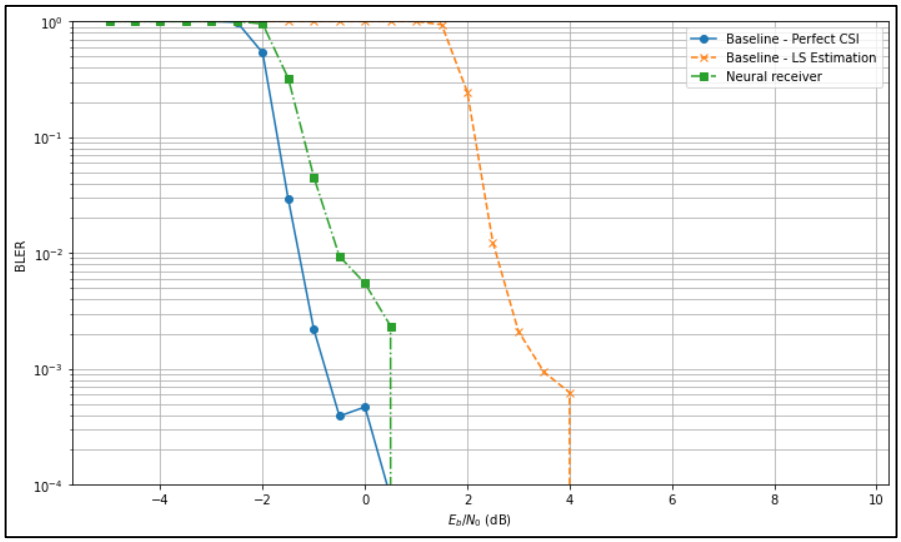

Figure 3.6: The output result of perfect CSI, LS estimation, and Neural receiver.

The graph above demonstrates how much higher the theoretical ratings of the Rx-NN receiver are than those of the LMMSE receiver for the LS channel. Even if just one example code is provided at a time, the CNN-based Rx-NN can almost match the performance of the LMMSE receiver (perfect channel). Since the practical LMMSE receiver requires two pilots to operate continuously in these circumstances, it performs very poorly with just one pilot. Even though the LMMSE has access to two pilots because of the wide Doppler shift range contained in the data at higher SINRs, the Rx-NN only requires one pilot to perform better than the LMMSE. Another aspect of this incredibly high performance is the encoded BER rates (Table No.3.2), which show that the LLRs generated by Rx-NN are good enough for an LDPC decoder. The LLRs' encoded BER rates are the same as the LMMSE receivers with full channel information, it is another element that makes their remarkable (adequate quality, optimal channel) quality. The encoded BER rates (Table No.3.3) demonstrate that the LLRs computed by Rx-NN are of appropriate quality for an LDPC decoder, which is another factor in this performance (perfect channel), since the encoded BER matches the quality of the LMMSE receiver with full channel knowledge. Exceptionally. The benefit of using a genuine LMMSE receiver is that even a practical LMMSE receiver cannot access the waterfall portion of the code, and when the

number of experimental tokens is reduced from two to one, Rx-NN performance is only marginally impacted. While all reference LMMSE receivers perform poorly due to the absence of interference mitigation features. When the encoded bit error rate (BER) is taken into account this is probably due to the fact that when calculating LLRs, the standard assignment factor assumes a white noise with a Gaussian distribution, while the somewhat high interference signal invalidates this assumption. While Rx-NN performs better than Reference receptors under intercellular interference The Rx-NN avoids making these assumptions since it implicitly learns the proper future behavior of noise based on the training data it receives, and interference distributions.

4. CONCLUSION

The advantages of full learning over AWGN channels were used in this study, although they were not quantified on wireless microchannel models. This paper attempts to close this gap by examining the end-to-end learning gains over the frequency and time-selective fading channel utilizing orthogonal frequency division multiplexing (OFDM). The modulation gains reported on the AWGN channels disappeared once it was realized that the receiver channel was not flawless. However, we also find an additional source of performance improvement. It originates from a neural network-based receiver Rx-NN that uses many subcarriers and OFDM codes, allowing to reduce orthogonal pilots without sacrificing the Bit Error Rate (BER) , As part of a supervised training effort, we examined a DL-based digital radio receiver that was created to meet the requirements of 5G wireless communication. It was taught using encoded bits and frequency domain antenna signals. We anticipated that performance would be enhanced by training a simulated chain of digital receivers as a single supervised system. This was the primary driving force behind this endeavor. contrasting the training of various minor receiver parts one at a time. As a result, the system can be instantaneously optimized for the job of retrieving the transmitted bits. Additionally, the neural network's architecture enables the least amount of learning for both optimal and predictable receiving systems. By doing so, he can learn to tackle a variety of difficult implicit identification issues with radio channels and equipment. We have built a completely deep convolutional neural network, known as -Rx-NN, that is trained to recognize encoded bits directly from frequency domain antenna signals in order to process and investigate the idea. Rx-NN has also been trained to handle a variety of 5G wireless network modification and piloting scenarios. In contrast to many similar efforts, convolutional input channels were created for neural network inputs that combined both known experimental codes and unknown data codes. As a result, when calculating the channel, Rx-NN was able to combine the data and the experimental code well. The results from 5G uplink and downlink data transmission simulation models demonstrate that the Rx-NN neural receiver performs better than conventional techniques. In addition, it outperformed a different neural network design in which channel estimation and equation were taken into account individually. We attribute the success of the Rx-NN neural receiver to efficient channel estimation and

equalization using the local symbol distribution and known constellation locations for unknown data symbols. In fact, some studies have shown that the intrinsic processing of Rx-NN receptors and repetitive receptors is somewhat comparable. It has also been shown that Rx-NN can effectively process non-Gaussian noise and interference over time. Since the main focus of this article is on the improvements in radio performance resulting from the use of deep learning, this work's lack of substantial study of computational complexity is one of its weaknesses. Even though we have looked at a number of methods to improve network performance, additional research is still required to develop these networks into slices of temporal neural networks. Furthermore, it is hardware-specific to compare total complexity with conventional receivers, and you should put more emphasis on latency and power usage than radio performance. Even if such analysis is outside the purview of this essay, it is an important topic for our subsequent study. Using an OFDM channel model that accounts for frequency selectivity and channel aging, we assessed neural receptor performance. Our findings demonstrate that a neural receptor acting on many sub transmitters and OFDM codes provides significantly lower BER rates while employing a small number of orthogonal pilots. Next, we demonstrate how reliable code detection is made possible without the need for orthogonal pilots thanks to the combined optimization of the neural transceiver. Productivity gains are possible since no renewable energy is lost when reference signals are sent.

5. FUTURE WORKS

In the future, this research can be expanded to exploit the gains from the application of deep learning techniques in 5G wireless communications. While knowing the receiver's various components has yielded some benefits, this can be extended to include the use of deep science techniques across all components rather than individual components where convolutional neural networks trained from start to finish can be used as a single piece which significantly reduces computational complexity Large and participate in the design of wireless communication networks in multiple input- multiple inputs (MIMO) instead of traditional methods and reduce the computational complexity of these methods and this can be an input for the sixth generation of wireless communication networks 6G. The fact that this research only contains a finite computational complexity study of the network that was utilized to create the Rx-NN neural receives is one of its limitations. Instead, the improvement in radio performance achieved through the use of deep learning is the main emphasis of this work, and future work of this study on conditioning may include the use of these networks to infer temporal neural network chips and use them to improve network efficiency since it can eliminate the need for channel guessing bookmarks and modulation removal and the associated overhead, we believe the jointly acquired transceiver is a very exciting component of post 5G communication systems.

REFERENCES

[1] Gawas, A. U. An overview on evolution of mobile wireless communication networks: 1G-6G. International Journal on Recent and Innovation Trends in Computing and Communication, 3(5), 3130-3133, (2015).

[2] Weldon, M. K. The future X network: a Bell Labs perspective. CRC press, (2016).

[3] Series, M. Minimum requirements related to technical performance for IMT-2020 radio interface (s). Report, 2410-0,

[4] Ji, H., Park, S., Yeo, J., Kim, Y., Lee, J., & Shim, B.. Ultra-reliable and low-latency communications in 5G downlink: Physical layer aspects. IEEE Wireless Communications, 25(3), 124-130, (2018).

[5] Zhang, H., Liu, N., Chu, X., Long, K., Aghvami, A. H., & Leung, V. C. Network slicing based 5G and future mobile networks: mobility, resource management, and challenges. IEEE communications magazine, 55(8), 138-145, (2017).

[6] Wu, Z., Lu, K., Jiang, C., & Shao, X. Comprehensive study and comparison on 5G NOMA schemes. IEEE Access, 6, 18511-18519, (2018).

[7] Wang, X., Kong, L., Kong, F., Qiu, F., Xia, M., Arnon, S., & Chen, G. Millimeter wave communication: A comprehensive survey. IEEE Communications Surveys & Tutorials, 20(3), 1616-1653, (2018).

[8] Zhang, F., & Wu, M. Hybrid analog-digital precoding for millimeter wave MIMO systems. In 2017 IEEE 17th International Conference on Communication Technology (ICCT) (pp. 69-73). IEEE, (2017, October).

[9] Larsson, E. G., Edfors, O., Tufvesson, F., & Marzetta, T. L. Massive MIMO for next generation wireless systems. IEEE communications magazine, 52(2), 186-195, (2014).

[10] Björnson, E., Hoydis, J., & Sanguinetti, L. Massive MIMO networks: Spectral, energy, and hardware efficiency. Foundations and Trends® in Signal Processing, 11(3-4), 154-655, (2017).

[11] Liyanage, M., Ahmad, I., Abro, A. B., Gurtov, A., & Ylianttila, M. (Eds.). A comprehensive guide to 5G security (p. 231). Hoboken: John Wiley & Sons, (2018).

[12] Meerasri, P., Uthansakul, P., & Uthansakul, M. Self-interference cancellation-based mutual-coupling model for full-duplex single-channel MIMO systems. International Journal of Antennas and Propagation, (2014).

[13] Muggleton, S. Alan Turing and the development of Artificial Intelligence. AI communications, 27(1), 3-10, (2014).

[14] Rich, E. Artificial intelligence and the humanities. Computers and the Humanities, 117-122, (1985).

[15] Cayamcela, M. E. M., & Lim, W. Artificial intelligence in 5G technology: A survey. In 2018 International Conference on Information and Communication Technology Convergence (ICTC) (pp. 860-865). IEEE, (2018, October).

[16] Alkhateeb, A., El Ayach, O., Leus, G., & Heath, R. W. Channel estimation and hybrid precoding for millimeter wave cellular systems. IEEE journal of selected topics in signal processing, 8(5), 831-846, (2014).

[17] Alkhateeb, A., Leus, G., & Heath, R. W. Limited feedback hybrid precoding for multi-user millimeter wave systems. IEEE transactions on wireless communications, 14(11), 6481-6494, (2015).

[18] Ren, Y., Wang, Y., Qi, C., & Liu, Y. Multiple-beam selection with limited feedback for hybrid beamforming in massive MIMO systems. IEEE Access, 5, 13327-13335, (2017).

[19] Singh, J., & Ramakrishna, S. On the feasibility of codebook-based beamforming in millimeter wave systems with multiple antenna arrays. IEEE transactions on Wireless Communications, 14(5), 2670-2683, (2015).

[20] Thomas, T. A., & Vook, F. W. Method for obtaining full channel state information for RF beamforming. In 2014 IEEE Global Communications Conference (pp. 3496-3500). IEEE, (2014, December).

[21] Hosoya, K. I., Prasad, N., Ramachandran, K., Orihashi, N., Kishimoto, S., Rangarajan, S., & Maruhashi, K. Multiple sector ID capture (MIDC): A novel beamforming technique for 60-GHz band multi-Gbps WLAN/PAN systems. IEEE Transactions on Antennas and Propagation, 63(1), 81-96, (2014).

[22] El Ayach, O., Rajagopal, S., Abu-Surra, S., Pi, Z., & Heath, R. W. Spatially sparse precoding in millimeter wave MIMO systems. IEEE transactions on wireless communications, 13(3), 1499-1513, (2014).

[23] Alkhateeb, A., Leus, G., & Heath, R. W. Compressed sensing based multi-user millimeter wave systems: How many measurements are needed?. In 2015 IEEE international conference on acoustics, speech and signal processing (ICASSP) (pp. 2909-2913). IEEE, (2015, April).

[24] Bogale, T. E., & Le, L. B. Beamforming for multiuser massive MIMO systems: Digital versus hybrid analog-digital. In 2014 IEEE Global Communications Conference (pp. 4066-4071). IEEE, (2014, December).

[25] Gupta, A., & Jha, R. K. A survey of 5G network: Architecture and emerging technologies. IEEE access, 3, 1206-1232, (2015).

[26] Larsson, E. G., Edfors, O., Tufvesson, F., & Marzetta, T. L. Massive MIMO for next generation wireless systems. IEEE communications magazine, 52(2), 186-195, (2014).

[27] Lu, L., Li, G. Y., Swindlehurst, A. L., Ashikhmin, A., & Zhang, R. An overview of massive MIMO: Benefits and challenges. IEEE journal of selected topics in signal processing, 8(5), 742-758, (2014).

[28] Gesbert, D., Hanly, S., Huang, H., Shitz, S. S., Simeone, O., & Yu, W. Multi-cell MIMO cooperative networks: A new look at interference. IEEE journal on selected areas in communications, 28(9), 1380-1408, (2010).

[29] Kuo, P. H., Kung, H. T., & Ting, P. A. Compressive sensing based channel feedback protocols for spatially-correlated massive antenna arrays. In 2012 IEEE Wireless Communications and Networking Conference (WCNC) (pp. 492-497). IEEE, (2012, April).

[30] O'Shea, T. J., Erpek, T., & Clancy, T. C. Deep learning based MIMO communications. arXiv preprint arXiv:1707.07980, (2017).

[31] Hijazi, H., Simon, E. P., Lienard, M., & Ros, L. Channel estimation for MIMO-OFDM systems in fast time-varying environments. In 2010 4th international symposium on communications, control and signal processing (ISCCSP) (pp. 1-6). IEEE, (2010, March).

[32] Simeone, O. A very brief introduction to machine learning with applications to communication systems. IEEE Transactions on Cognitive Communications and Networking, 4(4), 648-664, (2018).

[33] O'shea, T., & Hoydis, J. An introduction to deep learning for the physical layer. IEEE Transactions on Cognitive Communications and Networking, 3(4), 563-575, (2017).

[34] Huang, H., Song, Y., Yang, J., Gui, G., & Adachi, F. Deep-learning-based millimeter-wave massive MIMO for hybrid precoding. IEEE Transactions on Vehicular Technology, 68(3), 3027-3032, (2019).

[35] Gao, X., Dai, L., Han, S., Chih-Lin, I., & Wang, X. Reliable beamspace channel estimation for millimeter-wave massive MIMO systems with lens antenna array. IEEE Transactions on Wireless Communications, 16(9), 6010-6021, (2017).

[36] Heath, R. W., Gonzalez-Prelcic, N., Rangan, S., Roh, W., & Sayeed, A. M. An overview of signal processing techniques for millimeter wave MIMO systems. IEEE journal of selected topics in signal processing, 10(3), 436-453, (2016).

[37] Agiwal, M., Roy, A., & Saxena, N. Next generation 5G wireless networks: A comprehensive survey. IEEE Communications Surveys & Tutorials, 18(3), 1617-1655, (2016).

[38] Gupta, A., & Jha, R. K. A survey of 5G network: Architecture and emerging technologies. IEEE access, 3, 1206-1232, (2015).

[39] Zheng, K., Yang, Z., Zhang, K., Chatzimisios, P., Yang, K., & Xiang, W. Big data-driven optimization for mobile networks toward 5G. IEEE network, 30(1), 44-51, (2016).

[40] Nguyen, D. D., Nguyen, H. X., & White, L. B. Reinforcement learning with network-assisted feedback for heterogeneous RAT selection. IEEE Transactions on Wireless Communications, 16(9), 6062-6076, (2017).

[41] Narudin, F. A., Feizollah, A., Anuar, N. B., & Gani, A. Evaluation of machine learning classifiers for mobile malware detection. Soft Computing, 20(1), 343-357, (2016).

[42] Hsieh, K., Harlap, A., Vijaykumar, N., Konomis, D., Ganger, G. R., Gibbons, P. B., & Mutlu, O. Gaia:{Geo-Distributed} Machine Learning Approaching {LAN} Speeds. In 14th USENIX Symposium on Networked Systems Design and Implementation (NSDI 17) (pp. 629-647), (2017).

[43] Xiao, W., Xue, J., Miao, Y., Li, Z., Chen, C., Wu, M., ... & Zhou, L. {Tux²}: Distributed Graph Computation for Machine Learning. In 14th USENIX Symposium on Networked Systems Design and Implementation (NSDI 17) (pp. 669-682), (2017).

[44] Paolini, M., & Fili, S. Mastering Analytics: How to benefit from big data and network complexity: An Analyst Report. RCR Wireless News, 20(80), 120, (2017).

[45] Zhang, C., Zhou, P., Li, C., & Liu, L. A convolutional neural network for leaves recognition using data augmentation. In 2015 IEEE International Conference on Computer and Information Technology; Ubiquitous Computing and Communications; Dependable, Autonomic and Secure Computing; Pervasive Intelligence and Computing (pp. 2143-2150). IEEE, (2015, October).

[46] Socher, R., Bengio, Y., & Manning, C. D. Deep learning for NLP (without magic). In Tutorial Abstracts of ACL 2012 (pp. 5-5), (2012).

[47] Zhu, H., Zhang, Y., Li, M., Ashok, A., & Ota, K. Exploring deep learning for efficient and reliable mobile sensing. IEEE Network, 32(4), 6-7, (2018).

[48] Wang, M., Cui, Y., Wang, X., Xiao, S., & Jiang, J. Machine learning for networking: Workflow, advances and opportunities. Ieee Network, 32(2), 92-99, (2017).

[49] Chang, Z., Wang, Y., Li, H., & Wang, Z. Complex CNN-based equalization for communication signal. In 2019 IEEE 4th International Conference on Signal and Image Processing (ICSIP) (pp. 513-517). IEEE, (2019, July).

[50] Shental, O., & Hoydis, J. " Machine LLRning": Learning to Softly Demodulate. In 2019 IEEE Globecom Workshops (GC Wkshps) (pp. 1-7). IEEE, (2019, December).

[51] Gao, X., Jin, S., Wen, C. K., & Li, G. Y. ComNet: Combination of deep learning and expert knowledge in OFDM receivers. IEEE Communications Letters, 22(12), 2627-2630, (2018).

[52] Samuel, N., Diskin, T., & Wiesel, A. Learning to detect. IEEE Transactions on Signal Processing, 67(10), 2554-2564, (2019).

[53] Ye, H., Li, G. Y., & Juang, B. H. Power of deep learning for channel estimation and signal detection in OFDM systems. IEEE Wireless Communications Letters, 7(1), 114-117, (2017).

[54] Zhao, Z., Vuran, M. C., Guo, F., & Scott, S. D. Deep-waveform: A learned OFDM receiver based on deep complex-valued convolutional networks. IEEE Journal on Selected Areas in Communications, 39(8), 2407-2420, (2021).

[55] Dörner, S., Cammerer, S., Hoydis, J., & Ten Brink, S. Deep learning based communication over the air. IEEE Journal of Selected Topics in Signal Processing, 12(1), 132-143, (2017).

[56] Cammerer, S., Aoudia, F. A., Dörner, S., Stark, M., Hoydis, J., & Ten Brink, S. Trainable communication systems: Concepts and prototype. IEEE Transactions on Communications, 68(9), 5489-5503, (2020).

[57] Downey, J., Hilburn, B., O'Shea, T., & West, N. Machine learning remakes radio. IEEE Spectrum, 57(5), 35-39, (2020).

[58] Gündüz, D., de Kerret, P., Sidiropoulos, N. D., Gesbert, D., Murthy, C. R., & van der Schaar, M. Machine learning in the air. IEEE Journal on Selected Areas in Communications, 37(10), 2184-2199, (2019).

[59] Stark, M., Aoudia, F. A., & Hoydis, J. Joint learning of geometric and probabilistic constellation shaping. In 2019 IEEE Globecom Workshops (GC Wkshps) (pp. 1-6). IEEE, (2019, December).

[60] Cammerer, S., Aoudia, F. A., Dörner, S., Stark, M., Hoydis, J., & Ten Brink, S. Trainable communication systems: Concepts and prototype. IEEE Transactions on Communications, 68(9), 5489-5503, (2020).

[61] O'shea, T., & Hoydis, J. An introduction to deep learning for the physical layer. IEEE Transactions on Cognitive Communications and Networking, 3(4), 563-575, (2017).

[62] Zhu, Z. R., Zhang, J., Chen, R. H., & Yu, H. Y. Autoencoder-based transceiver design for OWC systems in log-normal fading channel. IEEE Photonics Journal, 11(5), 1-12, (2019).

[63] Karanov, B., Chagnon, M., Thouin, F., Eriksson, T. A., Bülow, H., Lavery, D., ... & Schmalen, L. End-to-end deep learning of optical fiber communications. Journal of Lightwave Technology, 36(20), 4843-4855, (2018).

[64] Dörner, S., Cammerer, S., Hoydis, J., & Ten Brink, S. Deep learning based communication over the air. IEEE Journal of Selected Topics in Signal Processing, 12(1), 132-143, (2017).

[65] Felix, A., Cammerer, S., Dörner, S., Hoydis, J., & Ten Brink, S. OFDM-autoencoder for end-to-end learning of communications systems. In 2018 IEEE 19th International Workshop on Signal Processing Advances in Wireless Communications (SPAWC) (pp. 1-5). IEEE, (2018, June).

[66] Kim, M., Lee, W., & Cho, D. H. A novel PAPR reduction scheme for OFDM system based on deep learning. IEEE Communications Letters, 22(3), 510-513, (2017).

[67] Balevi, E., & Andrews, J. G. One-bit OFDM receivers via deep learning. IEEE Transactions on Communications, 67(6), 4326-4336, (2019).

[68] Honkala, M., Korpi, D., & Huttunen, J. M. DeepRx: Fully convolutional deep learning receiver. IEEE Transactions on Wireless Communications, 20(6), 3925-3940, (2021).

[69] Ye, H., Li, G. Y., & Juang, B. H. Deep learning based end-to-end wireless communication systems without pilots. IEEE Transactions on Cognitive Communications and Networking, 7(3), 702-714, (2021).

[70] Shannon, C. E. A mathematical theory of communication. The Bell system technical journal, 27(3), 379-423, (1948).

[71] Nisioti, E., & Thomos, N. Design of capacity-approaching low-density parity-check codes using recurrent neural networks. arXiv preprint arXiv:2001.01249, (2020).

[72] Berrou, C., Glavieux, A., & Thitimajshima, P. Near Shannon limit error-correcting coding and decoding: Turbo-codes. 1. In Proceedings of ICC'93-IEEE International Conference on Communications (Vol. 2, pp. 1064-1070). IEEE, (1993, May).

[73] Zaidi, A., Athley, F., Medbo, J., Gustavsson, U., Durisi, G., & Chen, X. 5G Physical Layer: principles, models and technology components. Academic Press, (2018).

[74] Narandzic, M., Kyosti, P., Meinila, J., Hentila, L., Alatossava, M., Rautiainen, T., ... & Thoma, R. S. Advances in" Winner" Wideband MIMO System-Level Channel Modelling. In The Second European Conference on Antennas and Propagation, EuCAP 2007 (pp. 1-7). IET, (2007, November).

[75] Qu, Z., & Djordjevic, I. B. Geometrically shaped 16QAM outperforming probabilistically shaped 16QAM. In 2017 European Conference on Optical Communication (ECOC) (pp. 1-3). IEEE, (2017, September).

[76] Qu, Z., & Djordjevic, I. B. Geometrically shaped 16QAM outperforming probabilistically shaped 16QAM. In 2017 European Conference on Optical Communication (ECOC) (pp. 1-3). IEEE, (2017, September).

[77] Kongara, G., He, C., Yang, L., & Armstrong, J. A comparison of CP-OFDM, PCC-OFDM and UFMC for 5G uplink communications. IEEE Access, 7, 157574-157594, (2019).

[78] Edfors, O., Sandell, M., Van de Beek, J. J., Wilson, S. K., & Borjesson, P. O. OFDM channel estimation by singular value decomposition. IEEE Transactions on communications, 46(7), 931-939, (1998).

[79] Barb, G., & Otesteanu, M. On the influence of delay spread in tdl and cdl channel models for downlink 5g mimo systems. In 2019 IEEE 10th Annual Ubiquitous Computing, Electronics & Mobile Communication Conference (UEMCON) (pp. 0958-0962). IEEE, (2019, October).

[80] Tang, P., Zhang, J., Shafi, M., Dmochowski, P. A., & Smith, P. J. Millimeter wave channel measurements and modelling in an indoor hotspot scenario at 28 GHz. In 2018 IEEE 88th Vehicular Technology Conference (VTC-Fall) (pp. 1-5). IEEE, (2018, August).

[81] Neumann, D., Wiese, T., & Utschick, W. Learning the MMSE channel estimator. IEEE Transactions on Signal Processing, 66(11), 2905-2917, (2018).

[82] 3GPP. Technical specification group radio access network; nr; physical channels and modulation (release 16), (2020).

[83] Shental, O., & Hoydis, J. " Machine LLRning": Learning to Softly Demodulate. In 2019 IEEE Globecom Workshops (GC Wkshps) (pp. 1-7). IEEE, (2019, December).

[84] He, K., Zhang, X., Ren, S., & Sun, J. Identity mappings in deep residual networks. In European conference on computer vision (pp. 630-645). Springer, Cham, (2016, October).

[85] Sifre, L., & Mallat, S. Rotation, scaling and deformation invariant scattering for texture discrimination. In Proceedings of the IEEE conference on computer vision and pattern recognition (pp. 1233-1240), (2013).

[86] Chollet, F. Xception: Deep learning with depthwise separable convolutions. In Proceedings of the IEEE conference on computer vision and pattern recognition (pp. 1251-1258), (2017).

[87] You, Y., Li, J., Reddi, S., Hseu, J., Kumar, S., Bhojanapalli, S., ... & Hsieh, C. J. Large batch optimization for deep learning: Training bert in 76 minutes. arXiv preprint arXiv:1904.00962, (2019).

[88] Loshchilov, I., & Hutter, F. Decoupled weight decay regularization. arXiv preprint arXiv:1711.05101, (2017).